



The critical role of aqueous-phase processes in aromatic-derived nitrogen-containing organic aerosol formation in cities with different energy consumption patterns

Yi-Jia Ma^{1,2,3}, Yu Xu^{2,3}, Ting Yang^{1,2,3}, Lin Gui^{1,2,3}, Hong-Wei Xiao^{2,3}, Hao Xiao^{2,3}, and Hua-Yun Xiao^{2,3}

¹School of Environmental Science and Engineering, Shanghai Jiao Tong University, Shanghai 200240, China

²School of Agriculture and Biology, Shanghai Jiao Tong University, Shanghai 200240, China

³Shanghai Yangtze River Delta Eco-Environmental Change and Management Observation and Research Station, Ministry of Science and Technology, National Forestry and Grassland Administration, Shanghai 200240, China

Correspondence: Yu Xu (xuyu360@sjtu.edu.cn)

Received: 18 August 2024 – Discussion started: 7 October 2024

Revised: 20 December 2024 – Accepted: 14 January 2025 – Published: 4 March 2025

Abstract. Nitrogen-containing organic compounds (NOCs) impact air quality and human health. Here, the abundance, potential precursors, and main formation mechanisms of NOCs in PM_{2.5} during winter were compared for the first time among Haerbin (dependent on coal for heating), Beijing (natural gas and coal as heating energy), and Hangzhou (no centralized heating policy). The total signal intensity of CHON⁺, CHN⁺, and CHON[−] compounds was highest in Haerbin and lowest in Hangzhou. Anthropogenic aromatics accounted for 73 %–93 % of all identified precursors of CHON⁺, CHN⁺, and CHON[−] compounds in Haerbin. Although the abundance of aromatic-derived NOCs was lower in Beijing than in Haerbin, aromatics were also the main contributors to NOC formation in Beijing. Hangzhou exhibited the lowest levels of aromatic precursors. Furthermore, non-metric multidimensional scaling analysis indicated an overall reduction in the impact of fossil fuel combustion on NOC pollution along the route from Haerbin to Beijing to Hangzhou. We found that aqueous-phase processes (mainly condensation, hydrolysis, or dehydration processes for reduced NOCs and mainly oxidation or hydrolysis processes for oxidized NOCs) can promote the transformation of precursors to produce NOCs, leading to the most significant increase in aromatic NOC levels in Haerbin (particularly on haze days). Reduced precursor emissions in Beijing and Hangzhou (the lowest) constrained the aqueous-phase formation of NOCs. The overall results suggest that the aerosol NOC pollution in coal-dependent cities is mainly controlled by anthropogenic aromatics and aqueous-phase processes. Thus, without effective emission controls, the formation of NOCs through aqueous-phase processes may still pose a large threat to air quality.

1 Introduction

Nitrogen-containing organic compounds (NOCs) are abundant reactive nitrogen species in aerosol particles, accounting for up to 40 %–80 % of total nitrogen deposition (Li et al., 2023; Xi et al., 2023; Yu et al., 2020). Clearly, aerosol NOCs can significantly contribute to the global nitrogen cycle (Li

et al., 2023; Cape et al., 2011). Moreover, the formation of secondary organic aerosols (SOAs) and light-absorbing organic aerosols (e.g., brown carbon) is also tightly associated with NOCs (Wang et al., 2024; Liu et al., 2023b; Zeng et al., 2021), thus affecting the radiative balance and air quality (Yuan et al., 2023; Jiang et al., 2023). In particular, certain NOCs, such as nitroaromatics and peroxyacyl nitrates, are

characterized as phytotoxins and potential carcinogens, posing threats to ecosystems and human health (Shi et al., 2023; Singh and Kumar, 2022; Huang et al., 2024). Therefore, understanding the characteristics, origins, and atmospheric processes of NOCs is essential for comprehending their climate and health effects.

Aerosol NOCs can be derived from primary emissions associated with anthropogenic activities and natural sources (Lin et al., 2023; Xu et al., 2020a; Wang et al., 2017; Song et al., 2018, 2022; Ma et al., 2024; Gui et al., 2024; Xu et al., 2024a). Secondary formation processes may play a more crucial role in the formation of NOCs in fine aerosol particles, which involve interactions among volatile organic compounds (VOCs), atmospheric oxidants, and reactive inorganic nitrogen species (Montoya-Aguilera et al., 2018; Perraud et al., 2012; Hallquist et al., 2009). For instance, laboratory studies have observed the formation of organic nitrates from the oxidation of isoprene and α -/ β -pinene by atmospheric oxidants and nitrogen oxides (NO_x) (Surratt et al., 2010; Rollins et al., 2012; Nguyen et al., 2015). Additionally, aqueous-phase reactions of NH_4^+ (or NH_3) with biogenic VOCs or carbonyl compounds have been suggested to be important mechanisms of reduced NOC (Re-NOC) formation (Abudumutailifu et al., 2024; Laskin et al., 2014; Li et al., 2019b; Liu et al., 2023b; Wang et al., 2024). However, understanding the origins, formation mechanisms, and environmental impacts of NOCs is hindered by the elusive and intractable molecular information regarding NOCs and their precursors.

Aerosol liquid water (ALW) can greatly increase the formation of aerosol NOCs by facilitating the conversion of water-soluble organic gases into particles and subsequently enabling aqueous-phase reactions (Li et al., 2019a; Lv et al., 2022; Liu et al., 2023b). Several observational studies have found a positive correlation between aerosol NOC abundance and either ALW or relative humidity (RH) (Jiang et al., 2023; Liu et al., 2023b; Xu et al., 2020b). In particular, it has been suggested that increased ALW levels can exacerbate winter haze in China (Wu et al., 2018; Hodas et al., 2014; Lv et al., 2022; Wang et al., 2021d; Liu et al., 2023b; Wang et al., 2021a; Li et al., 2019a). Presumably, precursors and ALW are the two key factors in the formation of aerosol NOCs. Haze environments have potentially high RH levels and large emissions of NOC precursors (Zheng et al., 2023; Nie et al., 2022; Liu et al., 2021; Wang et al., 2021a). Moreover, in Chinese cities with different energy consumption (e.g., coal, biomass, and natural gas) for winter heating (Zhang et al., 2021b, 2023b; Yang et al., 2024c), the types and emission intensities of pollutants released from different heating sources are expected to vary considerably (Bond et al., 2006; Stockwell et al., 2015; Křůmal et al., 2019). However, the potential effects of ALW in the formation of NOCs in Chinese cities with different energy consumption during winter, particularly in haze periods, are not well documented. Moreover, the roles of ALW-related NOC formation processes in the

formation of haze in cities with different energy consumption types also remain largely unknown.

In this study, we present the measurements of the NOCs and other chemical compositions in $\text{PM}_{2.5}$ collected from three cities (Haerbin, Beijing, and Hangzhou) with different energy consumption during winter. The specific objectives of this study were the following: (1) to investigate the differences in the abundance, composition, and major precursors of NOCs in cities with different energy consumption, especially on polluted days, and (2) to elucidate the potential effects of aqueous-phase processes on the formation of oxidized NOCs (Ox-NOCs) and reduced NOCs (Re-NOCs) during winter (particularly on polluted days) in cities with different energy consumption. The research findings are expected to provide valuable implications for the mitigation of aerosol NOC pollution in urban environments.

2 Materials and methods

2.1 Study site description and sample collection

The study sites are located in three urban areas, including Haerbin (HEB, i.e., Harbin; 126.64° E, 45.77° N), Beijing (BJ; 116.41° E, 40.04° N), and Hangzhou (HZ; 120.16° E, 30.30° N) (Fig. S1 in the Supplement). The city of HEB, with a population of 9.95 million, is situated in the northeastern region of China. It relies heavily on coal for centralized heating during winter. The rapid urbanization and increased coal consumption have significantly deteriorated air quality in HEB in recent years (Ma et al., 2020). In contrast, BJ has largely shifted towards the utilization of cleaner energy sources (e.g., natural gas) for centralized heating in recent years, particularly following the implementation of the Beijing 2013–2017 Clean Air Action Plan (Vu et al., 2019; Yuan et al., 2023). HZ, situated within the Yangtze River Delta, is exempt from the necessity of heating due to the relatively mild winter climate (average temperature of 6.6 ± 2.4 °C during the sampling period; Table S1). Clearly, the distinctive energy consumption patterns observed in these three cities during winter provide a valuable opportunity to examine the impact of various precursors and aqueous-phase processes on aerosol NOC formation.

Sample collection was carried out simultaneously in three cities from 16 December 2017 to 14 January 2018. $\text{PM}_{2.5}$ samples were collected every 2 or 3 d with a duration of 24 h onto prebaked quartz fiber filters (Pallflex, Pall Corporation, USA) using a high-volume air sampler (Series 2031, Laoying, China). One blank sample was collected at each sampling site. A total of 39 samples were collected, all of which were stored at -30 °C. Meteorological data (e.g., temperature, relative humidity (RH), and wind speed) together with concentrations of various pollutants (e.g., SO_2 and NO_2) were obtained from nearby environmental stations. In China, according to the air quality index (MEEPRC, 2012), a pollution day is defined as a day with a 24 h average $\text{PM}_{2.5}$ con-

centration above $75 \mu\text{g m}^{-3}$. This standard has also been used in other studies performed in China (Zhang and Cao, 2015; Xu et al., 2024b; Yan et al., 2024), showing that the sampling periods were classified as either “clean” or “haze” based on whether the daily average concentration of $\text{PM}_{2.5}$ was below or above $75 \mu\text{g m}^{-3}$.

2.2 Chemical analysis

The extraction and analysis methods for NOCs were consistent with those described in our recent publication (Ma et al., 2024). Briefly, a portion of each filter was extracted with methanol (LC-MS grade, CNW Technologies Ltd.) using sonication in an ice bath ($\sim 4^\circ\text{C}$). The extracts were filtered through a $0.22 \mu\text{m}$ polytetrafluoroethylene syringe filter and then concentrated to $300 \mu\text{L}$ under a gentle stream of nitrogen gas. The concentrated extracts underwent composition analysis via an ultra-performance liquid chromatography coupled with a quadrupole time-of-flight mass spectrometer equipped with an electrospray ionization (ESI) source (UPLC-ESI-QToFMS, Waters ACQUITY Xevo G2-XS) (Wang et al., 2021c; Ma et al., 2024). This analysis was done in both ESI+ and ESI− modes. The organic compounds were separated on an ACQUITY HSS T3 column ($2.1 \times 100 \text{ mm}$, $1.8 \mu\text{m}$ particle size, Waters) with an 18 min gradient elution. The mobile phases comprised ultrapure water with 0.1 % formic acid (A) and methanol with 0.1 % formic acid (B). Gradient elution was conducted according to the following protocol: 1 % B was held for 1.5 min, followed by an increase to 54 % B over a period of 6.5 min. Thereafter, B was increased to 95 % over a period of 3 min. After reaching 100 % B in 1 min, this state was maintained for 3 min. Finally, the concentration was returned to 1 % B in 0.5 min and held for 2.5 min. More detailed information about the UPLC-ESI-QToFMS analysis can be found in Sect. S1. Due to uncertainties in ionization efficiencies for different compounds (Ditto et al., 2022; Yang et al., 2023), an intercomparison (mainly compared among samples within this study) of compound relative abundance was conducted without accounting for differences in ionization efficiency in the present study. This consideration was consistent with previous studies (Xu et al., 2023; Jiang et al., 2022; Ma et al., 2024).

Another filter portion was ultrasonically extracted using Milli-Q water ($\sim 4^\circ\text{C}$ ice bath) to analyze the concentrations of inorganic ions and organic acids. The inorganic ions (e.g., NO_3^- , SO_4^{2-} , Cl^- , Ca^{2+} , Mg^{2+} , Na^+ , and NH_4^+) and organic acids (e.g., formic acid, acetic acid, oxalic acid, succinic acid, glutaric acid, and methanesulfonic acid) were quantified using an ion chromatograph system (Dionex Aquion, Thermo Scientific, USA), as described previously (Xu et al., 2022b; Yang et al., 2024b).

2.3 Compound categorization and precursor identification

The identified molecular formulas via UPLC-ESI-QToFMS were categorized into different compound classes based on their elemental compositions, which included CHO−, CHON−, CHONS−, and CHOS− in ESI− mode and CHO+, CHON+, and CHN+ in ESI+ mode (Ma et al., 2024). Unless otherwise indicated, the molecular formulas presented in the article refer to neutral molecules. The “−” and “+” symbols denote the detection ion modes, which correspond to ESI− and ESI+ modes, respectively. Here, we mainly focus on NOCs (i.e., CHN+, CHON+, and CHON− compounds) (Ma et al., 2024; Jiang et al., 2022; Wang et al., 2017). The carbon oxidation state (OS_C) and double bond equivalent (DBE) were calculated to indicate the oxidation level and unsaturation degree of the organics, respectively (Sect. S2) (Kroll et al., 2011; Ma et al., 2024). Additionally, the modified aromaticity index (AI_mod) and aromaticity equivalent (X_C) were used to evaluate aromaticity of organics (Koch and Dittmar, 2006), as detailed in Sect. S2.

The potential precursors of NOCs were identified based on the methodology described in previous studies (Nie et al., 2022; Guo et al., 2022; Jiang et al., 2023). The classification of CHON+ and CHON− compounds was refined into the following categories: aliphatic-, heterocyclic-, and aromatic-derived Re-NOCs and isoprene-, monoterpene-, aliphatic-, and aromatic-derived Ox-NOCs. Moreover, CHN+ compounds were classified into aliphatic, monoaromatic, and polyaromatic CHN+ compounds (Wang et al., 2021b; Yassine et al., 2014). A detailed description of the revised workflow for classifying NOCs according to potential precursors is provided in Sect. S3 and Fig. S2.

2.4 Classification of potential pathways for NOC formation

To identify potential aqueous-phase processes for aerosol NOC formation, we screened precursor–product pairs from the organic compounds that have been detected (Su et al., 2021; Xu et al., 2023; Jiang et al., 2023). The reaction pathways of Re-NOCs (mainly CHON+ compounds in this study) were refined into the following categories: condensation (cond_N), hydrolysis (hy_N), dehydration (de_N), cond_hy_N (involving cond_N and hy_N), cond_de_N (involving cond_N and de_N), hy_de_N (involving hy_N and de_N), cond_hy_de_N (involving cond_N, hy_N and de_N), and unknown_N (unknown processes) formation pathways (Fig. S3 and Table S4) (Sun et al., 2024; Abudumutailifu et al., 2024; Laskin et al., 2014; Liu et al., 2023c). Another significant class of Re-NOCs is the CHN+ compounds. Their potential formation mechanisms include cond_N, de_N, cond_de_N, and other unidentified (unknown_N) pathways (Fig. S4 and Table S4) (Abudumutailifu et al., 2024; Laskin et al., 2014; Liu et al., 2023c). In addition, the reaction

pathways of Ox-NOCs (mainly CHON– compounds in this study) were refined into the following categories: ox_N, hy_N, ox_hy_N (involving ox_N and hy_N), and other unidentified (unknown_N) pathways (Jiang et al., 2023; Su et al., 2021) (Fig. S5 and Table S4). A detailed overview of the methodologies employed to discern potential NOC formation pathways is shown in Sect. S4, Table S4, and Figs. S3–S5.

It is important to acknowledge the potential limitations in the categorization methodology of NOC formation pathways described above. This is because the approach applied here and in previous studies (Jiang et al., 2023; Su et al., 2021) may classify NOCs as products of aqueous-phase reactions from primary emissions. Accordingly, our results can be regarded as a maximal potential (or an upper limit) for NOC generation from aqueous-phase reactions. In particular, certain reaction pathways (e.g., oligomerization) were not included in this study due to the complexity of the atomic changes involved, which could not be effectively characterized using the “precursor–product pairs” approach. In this study, NOCs produced from the reaction pathways identified by the abovementioned classification methodology can explain 76 % of CHON+ compounds, 61 % of CHN+ compounds, and 65 % of CHON– compounds. Thus, the classification of potential pathways for NOC formation was representative, at least in this study.

2.5 More parameter calculations and data analysis

A thermodynamic model (ISORROPIA II) was used to estimate the ALW concentration and pH value, as described in previous studies (Xu et al., 2020b, 2023, 2022c). Ambient hydroxyl radical ($\bullet\text{OH}$) concentrations were predicted using empirical formulas proposed by Ehhalt and Rohrer (2000), which were reported in detail in our previous field observations (Liu et al., 2023a; Lin et al., 2023). The ventilation coefficient (VC) is an indicator of the potential for atmospheric dilution of pollutants, which was calculated by multiplying the wind speed by the planetary boundary layer height (PBLH) (Gani et al., 2019).

Non-metric multidimensional scaling (NMDS) was employed to visualize the distributions of NOCs (CHON+, CHN+, and CHON– compounds) in two dimensions, based on Bray–Curtis distances (Chao et al., 2006). The stress values ranged from 0.03 to 0.11 (less than 0.2, Table S5) in our analysis, indicating that the differences among samples can be well represented in the two-dimensional pattern. To further assess the influence of anthropogenic emissions and aqueous-phase processes on the distribution of NOCs, the envfit function in the R package vegan (Oksanen, 2010) was utilized. Furthermore, the Spearman rank correlation, a non-parametric measure with less sensitivity to outliers and independent of data distribution assumptions, was employed to examine the association patterns between NOCs and the parameters related to anthropogenic emissions and aqueous-phase processes (Kellerman et al., 2014).

3 Results and discussion

3.1 Overview of pollution and aerosol NOC characteristics in different cities

Figure 1a–c and Table S1 show the variations in major gaseous pollutants, $\text{PM}_{2.5}$, and its major compositions, as well as meteorological parameters in three Chinese cities with different energy consumptions during winter. The average $\text{PM}_{2.5}$ concentration in HEB was $90.6 \pm 62.4 \mu\text{g m}^{-3}$, which was significantly higher than that observed in BJ ($52.7 \pm 51.4 \mu\text{g m}^{-3}$) and HZ ($69.1 \pm 29.6 \mu\text{g m}^{-3}$). Similarly, the concentrations of SO_2 and non-sea-salt (nss-Cl^-) were higher in HEB than in BJ and HZ. In addition, a lower $\text{NO}_3^- / \text{SO}_4^{2-}$ mass ratio (Table S1) was found in HEB. SO_2 and nss-Cl^- have been suggested to be typical pollutants emitted from coal combustion during winter in cities (Zhao and Sun, 1986; Streets and Waldhoff, 2000). The low $\text{NO}_3^- / \text{SO}_4^{2-}$ mass ratio can indicate a predominance of stationary sources (e.g., coal combustion) (Wang et al., 2006; Arimoto et al., 1996; Xiao and Liu, 2004). These results suggest that coal combustion during the winter heating season in HEB may significantly contribute to severe $\text{PM}_{2.5}$ pollution. This consideration can also be supported by the highest coal consumption in HEB in 2017–2018 (Fig. 1d). Due to the large-scale use of clean energy (i.e., natural gas) in BJ (Fig. 1e), the coal consumption in BJ was the lowest (Fig. 1d). This resulted in the lowest pollutant levels in BJ. From clean to polluted days, HEB and BJ showed larger increases in pollutant levels (e.g., $\text{PM}_{2.5}$, SO_2 , and CO), followed by HZ. Thus, the release of pollutants caused by the use of fossil fuels for centralized heating in winter (only occurred in HEB and BJ) was undoubtedly one of the important factors contributing to the generation of haze in HEB and BJ.

Figure 1f and g show the average signal intensity distributions of organic compounds detected in $\text{PM}_{2.5}$ across sampling periods in different cities. The detailed mass spectra of organic compounds detected in ESI+ and ESI– are shown in Fig. S6. CHN_{1+} ($n = 437\text{--}448$) compounds were the main CHN molecules measured in ESI+ mode in all cities (Fig. 1f and Table S6), the signal intensity of which accounted for over 77 % of the total $\text{CHN}_{1\text{--}3+}$ signal intensity. Similarly, CHON_{1+} compounds ($n = 398\text{--}421$) dominated in $\text{CHON}_{1\text{--}3+}$ molecules, with a higher signal intensity than $\text{CHON}_{2\text{--}3+}$ (Fig. 1f and Table S6). The high abundances of CHN_{1+} and CHON_{1+} compounds in NOCs were similar to previous reports about the NOC characteristics of urban aerosols (He et al., 2024; Abudumutailifu et al., 2024). The signal intensity fractions (40 %–77 %) of CHN+ compounds in total NOCs in these three cities were higher than those observed (8.20 %–17.47 %) during winter in Ürümqi, where the same NOC analysis method was conducted (Ma et al., 2024). However, the signal intensity fractions of CHON+ compounds in total NOCs were lower in these three cities (23 %–60 %) than in Ürümqi (over 82.53 %) (Ma et al., 2024). More

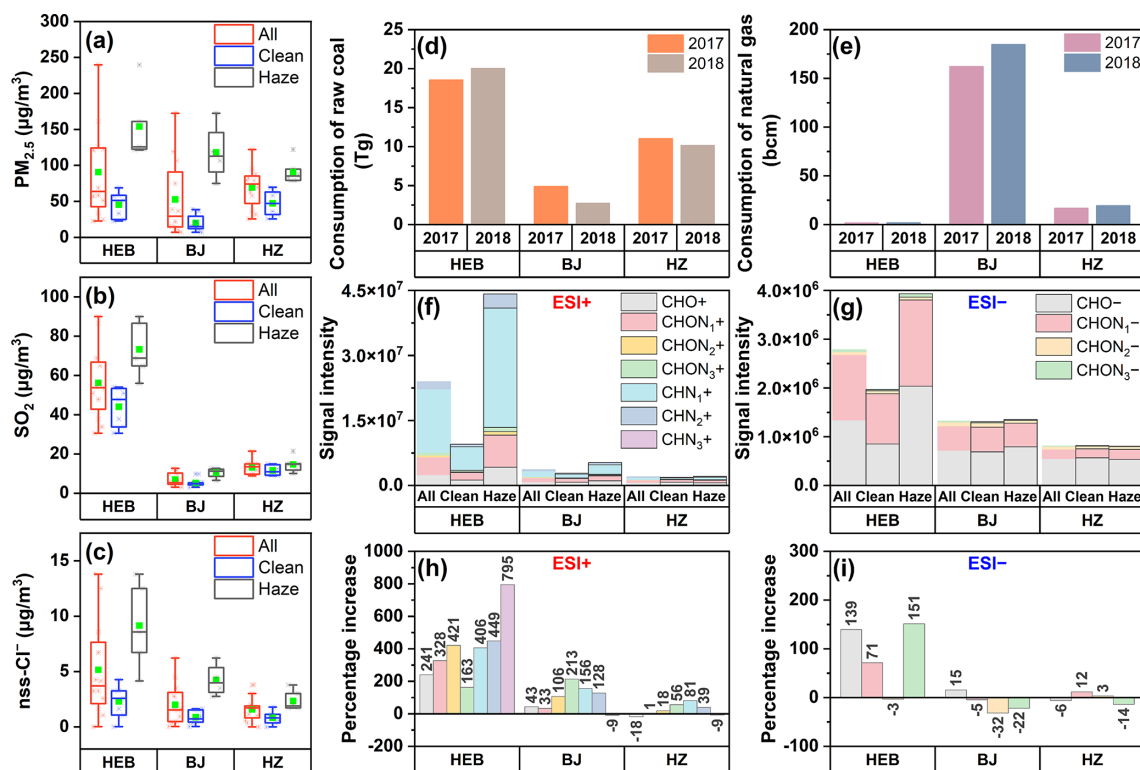


Figure 1. Box-and-whisker plots showing variations in the concentration of (a) $PM_{2.5}$, (b) SO_2 , and (c) $nss-Cl^-$ in all (red), clean (blue), and haze (gray) periods in different cities. Each box encompasses the 25th–75th percentiles. Whiskers are the 5th and 95th percentiles. The green squares and solid lines inside boxes indicate the mean and median values. The consumption of (d) raw coal and (e) natural gas in 2017 and 2018 in different cities was obtained from the local statistical yearbooks. Average distributions in the signal intensity of species detected in $PM_{2.5}$ collected during different winter periods in different cities in (f) ESI+ and (g) ESI– modes. Percentage variations in the signal intensity of each subgroup from clean to haze periods in different cities in (h) ESI+ and (i) ESI– modes.

frequent biomass burning and the relatively dry climate in Ürümqi (northwestern China) (Ma et al., 2024) may result in different sources and formation processes of NOCs compared to this study. The signal intensity of these NOCs detected in ESI+ mode varied across cities, with the highest CHN+ and CHON+ signal intensities in HEB, followed by BJ and HZ. Moreover, we found that the total signal intensities of CHN+ and CHON+ compounds increased by 382 % in HEB from clean to haze periods, followed by an increase of 102 % in BJ and an increase of 31 % in HZ (Fig. 1h and Table S6). This variation pattern of CHN+ and CHON+ compounds from clean to haze periods was similar to that of the pollutants mentioned previously (Fig. 1a–c). Given the high sensitivity of ESI+ mode to protonatable species, reduced species (e.g., amine- and amide-like compounds) were expected to predominate the NOCs (Han et al., 2023; Wang et al., 2018), the formation of which was highly related to precursor emission level, aerosol acidity, and ALW concentrations (Kuwata and Martin, 2012; Vione et al., 2005; Yang et al., 2024a; Xu et al., 2020b). Thus, these results suggest that there may be significant differences in the sources, precursor

emission intensity, or main formation pathways of NOCs in cities with different energy consumptions.

The number of NOCs identified in ESI– (296–301 molecules excluding sulfur-containing compounds; Table S7) was found to be lower than that observed in ESI+ (1346–1361) (Table S6). This finding was similar to previous observations about NOCs of urban organic aerosols in Beijing, Mainz, Changchun, Guangzhou, and Shanghai (Wang et al., 2021b; Wen et al., 2023; Wang et al., 2018). $CHON_1-$ compounds were the main NOC molecules in ESI– mode in all cities (Fig. 1g and Table S7). The average signal intensity of $CHON-$ compounds was highest in HEB, followed by BJ and HZ. Moreover, the outbreak of $CHON_{1-3}$ signal intensity during polluted periods was found in HEB, whereas insignificant increases occurred in BJ and HZ (Fig. 1i). Deprotonated NOCs with oxidized nitrogen-functional groups, such as nitro ($-NO_2$) or nitrooxy ($-ONO_2$) groups, are more sensitive to the ESI– mode (Wang et al., 2017; Jiang et al., 2023; Yuan et al., 2023). Clearly, the formation of aerosol $CHON-$ compounds was largely dependent on atmospheric oxidation capacity and gas- and aqueous-phase reactions (Ng et al., 2017; Shi et al., 2020, 2023). Thus, the differences

in CHON[−] compound abundance in different polluted periods and cities together with the spatiotemporal changes in CHN⁺ and CHON⁺ abundances mentioned previously were likely attributed to variations in sources, mechanisms, or key influencing factors of NOC formation in these three cities, which will be further discussed in the following sections.

3.2 Potential precursors of aerosol NOCs in different cities

Figure 2 presents the average signal intensity percentage and signal intensity distributions of different NOCs from various precursors in different cities during winter. Aromatic-, heterocyclic-, and aliphatic-derived Re-NOCs together accounted for more than 74 % (74 %–79 %) of the total signal intensity of CHON⁺ compounds in the three studied cities (Fig. 2a–c and Table S8). Specifically, the proportion of the aromatic-derived CHON⁺ signal intensity in the total CHON⁺ signal intensity was much higher in HEB (73 %) than in BJ (33 %), with the lowest proportion observed in HZ (23 %) (Fig. 2a–c). Furthermore, we observed that aromatic CHN⁺ compounds (mono- and polyaromatics) dominated the total CHN⁺ compounds in both number and abundance in all investigated cities (Table S9 and Fig. 2d–f). The average signal intensity percentage and signal intensity of aromatic CHN⁺ compounds were also highest in HEB (Fig. 2d–f and k). The calculated AI_{mod} values for CHON⁺ and CHN⁺ compounds were higher in HEB than in BJ and HZ (Table S10), which further indicated a higher aromaticity of these NOCs in HEB. It has been suggested that coal combustion can release a large amount of aromatic compounds (Zhang et al., 2023a), which potentially increased NOC aromaticity (Yuan et al., 2023). Thus, the higher signal proportion of aromatic-derived Re-NOCs in HEB can be explained by the higher coal combustion emissions during winter. In contrast, the use of clean energy during the central heating season in BJ and the reduced emissions in HZ without central heating weakened the formation of aerosol aromatic NOCs.

CHON[−] compounds were also primarily dominated by aromatic-derived Ox-NOCs in all three cities, accounting for more than 73 % (73 %–90 %) of the total signal intensity of CHON[−] compounds, on average (Fig. 2g–i). This finding was consistent with field observations conducted in other Chinese cities such as Shanghai, Changchun, Guangzhou, and Wangdu during winter (Wang et al., 2021b; Jiang et al., 2023). The abundance of aromatic-derived Ox-CHON[−] compounds and the AI_{mod} value of CHON[−] were highest in HEB and decreased sequentially in BJ and HZ (Fig. 2l and Table S10), further indicating our previous consideration that coal combustion heating in HEB can lead to higher NOC pollution. It is worth noting that the percentage of total signal intensity of Ox-NOCs with biogenic VOCs (BVOCs) as precursors was less than 3 % (Fig. 2g–i and Table S8). This can be partly supported by the previous observations showing that anthropogenic VOCs (AVOCs) were the main contribu-

tors to the formation of Ox-NOCs (e.g., organic nitrates) in urban areas in China (Wang et al., 2021b; Jiang et al., 2023). The overall results suggest the significant role of AVOCs in the formation of NOCs in all investigated cities, particularly in HEB.

From clean to haze periods, the signal intensities of all aromatic-derived CHON compounds increased significantly in HEB (Figs. 2a, j, g, l and S7). In contrast, the signal intensities of aromatic-derived CHON compounds in BJ and HZ showed an insignificant increase during haze periods. In addition, the average values of O/C_w and OS_{C_w} for CHON⁺ and CHON[−] compounds were higher in HEB than in BJ (second highest) and HZ, and their increases from clean to haze periods were also greater in HEB (Table S10). Concurrently, the O/C_w ratio of aerosol NOCs in HEB was observed to be higher than that of coal-derived aerosols (Song et al., 2018). Heald et al. (2010) previously demonstrated that oxidation processes can lead to an increase in the O:C ratio of organic aerosols. These results indicated that aerosol NOCs in HEB were more oxidized aromatics (or aged aromatics), particularly during haze. The average N/C_w ratios of CHON⁺ and CHON[−] compounds in HEB (0.13 and 0.15, respectively) (Table S10) were higher than those of CHON⁺ (0.079) and CHON[−] (0.07) compounds in aerosols directly emitted from coal combustion (Song et al., 2022, 2018). The N/C_w ratios were also higher in HEB than in BJ and HZ and increased during hazy days (0.13 for CHON⁺ and 0.16 for CHON[−] in hazy days in HEB). It has been suggested that the N/C_w ratio of CHON[−] compounds tended to increase (from 0.109 to 0.119) after aging of fuel-combustion-derived aerosols (Zhao et al., 2022). Thus, these results, combined with previous analysis of potential precursors for NOCs, suggest that anthropogenic precursor emissions and their atmospheric transformation to form CHON compounds were stronger in HEB than in BJ and HZ. Moreover, considering that the emission intensity of precursors during clean and hazy days may not significantly change, secondary processes may significantly promote the formation of NOCs in HEB during hazy days (the most significant increase in NOC abundance). However, this promoting effect during hazy days was insignificant in BJ and HZ (lower increase in NOC abundance).

3.3 Main factors influencing aerosol NOC formation in different cities

As discussed in the previous section, the results indicated that AVOCs play a significant role in the formation of NOCs. Furthermore, secondary processes may contribute to NOC formation to varying extents in different cities. This section provides a detailed discussion of the key factors influencing the molecular distribution of NOCs. First, a Spearman correlation analysis was performed to examine the relationship between various parameters and NOCs (Figs. 3 and S8–S12). The peak intensity of most CHON⁺ compounds (mainly aro-

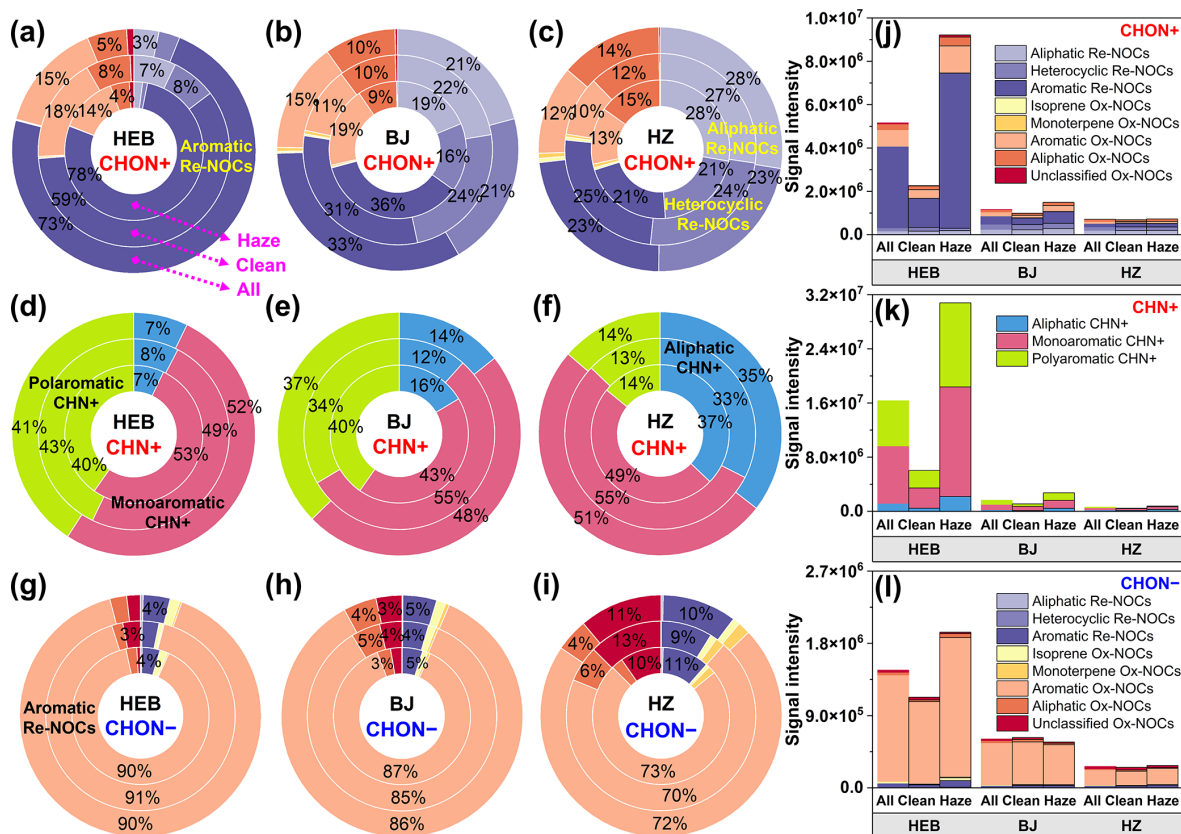


Figure 2. Average percentage distributions of signal intensities for (a–c) CHON+, (d–f) CHN+, and (g–i) CHON– compounds from various sources in PM_{2.5} collected from different cities during winter. Average signal intensity distributions for (j) CHON+, (k) CHN+, and (l) CHON– compounds from various sources in PM_{2.5} collected from different cities during winter.

matics, as mentioned previously) showed a strong correlation ($P < 0.01$) with the concentrations of combustion-source-related tracers (e.g., SO₂, nss-Cl⁻, nss-K⁺, CO, and NO₂) (Zhao and Sun, 1986; Streets and Waldhoff, 2000; Shen et al., 2009; Zhang et al., 2011; Mafusire et al., 2016; Liu et al., 2019; Zhang et al., 2021a; Wang et al., 2020) in HEB (Figs. 3a and S8a–d). Although there was a significant correlation ($P < 0.05$) between most CHON+ compounds and those combustion source indicators in BJ, the strength of this correlation was weaker in BJ than in HEB (Figs. 3e and S8f–i). However, similar significant correlations between them were not observed in HZ (Figs. 3i and S8k–n). Thus, the greatest contribution of anthropogenic activities to the formation of CHON+ compounds in winter was in HEB (central heating with coal), followed by BJ (central heating with coal and natural gas) and HZ (without central heating). Most of the CHN+ and CHON– compounds showed a similar spatial response pattern to those anthropogenic activities (Figs. S9 and S10). These results are consistent with the previous analysis of NOC precursors (Fig. 2), which concluded that the intensity of anthropogenic pollutant emissions in cities with different energy consumption was an important factor affect-

ing the formation of NOCs and causing spatial differences in NOC abundance.

Furthermore, we found that the peak intensities of most CHON+, CHN+, and CHON– compounds (mainly aromatics) were significantly correlated ($P < 0.01$) with the concentrations of ALW, NH₄⁺, oxalic acid, and SO₄²⁻ (Figs. 3b–d, S8e, and S11–S12) in HEB. The correlations between these NOCs and parameters weakened in BJ and disappeared in HZ (Figs. 3, S8, and S11–S12). It is generally accepted that SO₄²⁻, NH₄⁺, and NO₃⁻ in fine aerosols are primarily formed through secondary processes (Gao et al., 2021; Wang et al., 2021d). NH₄⁺ can serve as a key reactant in the formation of aerosol NOCs (e.g., “carbonyl-to-imine” transformation) in the aqueous phase (Laskin et al., 2014; Lee et al., 2013; Li et al., 2019b). Oxalic acid (C₂H₂O₄) has been identified as a marker (defined by Nozière et al., 2015) for aqueous-phase SOAs (Xu et al., 2022a; Chen et al., 2021). Additionally, numerous laboratory and field observational studies have shown that ALW can promote the formation of NOCs (Lv et al., 2022; Liu et al., 2023b; Jimenez et al., 2022; Jiang et al., 2023). Thus, these results indicate that aqueous-phase processes can significantly promote the formation of NOCs in HEB. However, as the precursor emission intensity gradu-

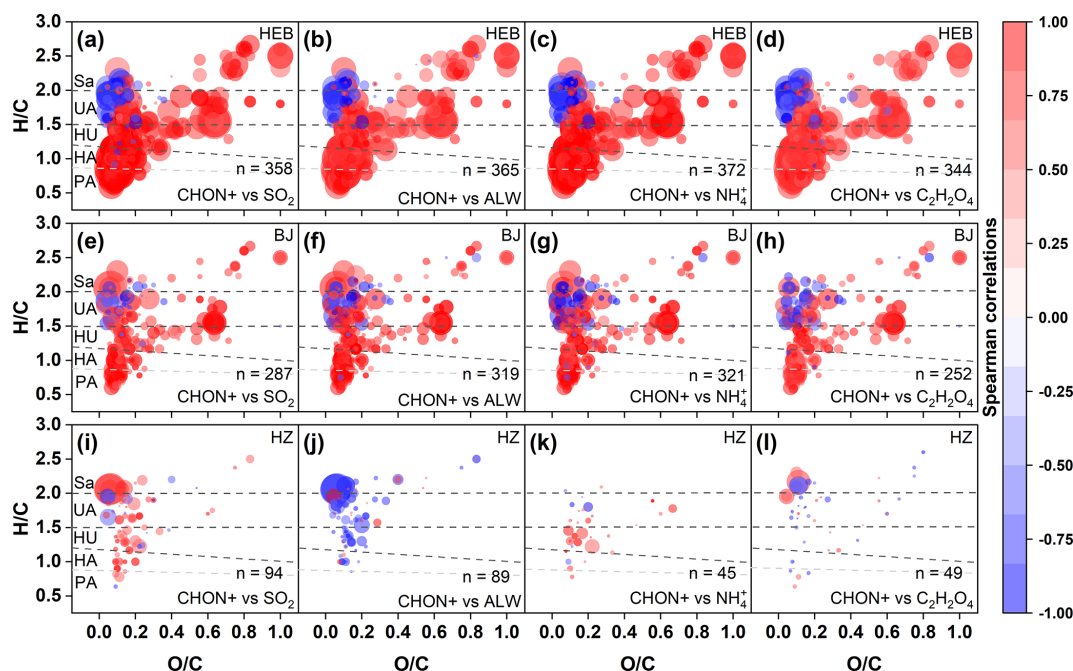


Figure 3. Spearman rank correlation coefficients (with $P < 0.01$ in HEB and $P < 0.05$ in BJ and HZ) of individual CHON+ molecules with selected parameters in (a–d) HEB, (e–h) BJ, and (i–l) HZ. The color scale indicates Spearman correlations between the intensity of individual CHON+ molecules and each parameter. The symbol n in the bottom right corner of each panel indicates the number of molecular formulas significantly correlated with the variables. The subgroups in the panels include polycyclic aromatic-like (PA), highly aromatic-like (HA), highly unsaturated-like (HU), unsaturated aliphatic-like (UA), and saturated-like (Sa) compounds.

ally decreased in BJ and HZ, this aqueous-phase promoting effect also decreased.

The NMDS analysis between various parameters and NOCs was conducted to further investigate the variations in key factors affecting the formation of NOCs from clean to haze days (Fig. 4). The formation of CHON+, CHN+, and CHON– compounds with higher AI_{mod} values (mainly aromatics, as mentioned previously) during haze days in HEB and BJ was closely associated with the factors indicating anthropogenic precursor emissions and aqueous-phase reaction processes. In contrast, the level of oxidants (i.e., O_3 and $\bullet OH$) played a more important role during clean days in HEB and BJ, driving more highly saturated NOC formation during clean days (Fig. 4). A reasonable explanation for this is that the solar radiation and $\bullet OH$ levels on polluted days were lower than those on clean days (Table S1). The impacts of various factors on the formation of aerosol NOCs showed a weak discrimination between haze and clean days in HZ (Fig. 4c, f and i). Laboratory studies have shown that reactive components (e.g., $\bullet OH$ and H_2O_2) in the aqueous phase can continuously convert low-solubility organics to form aqueous-phase SOAs (Chen et al., 2008; Huang et al., 2011; Dong et al., 2021). Field observations also suggested that precursors (most of them are aromatic compounds) released from the combustion of fossil fuels significantly contributed to the aqueous SOA formation (> 50 % total molecules) (Xu

et al., 2022a) through the rapid aqueous-phase conversion of primary organic aerosol (POA) to SOAs at high RH (Wang et al., 2021a). This implies that higher precursor abundance can drive more aerosol NOC formation via aqueous-phase processes. As mentioned previously, the emission intensity of precursors decreased sequentially from HEB to BJ and then to HZ. Moreover, the ALW concentrations were much higher on polluted days than on clean days in three investigated cities. The rising ALW during the pollution period and the quiescent steady state of the atmosphere favored the formation of SOAs from anthropogenic emission precursors (Guo et al., 2014; He et al., 2018). Thus, the above discussion can suggest that the spatial differences in precursor emission intensity (higher in HEB) and enhancement of aqueous-phase processes on polluted days were the main factors leading to the differences in the proportion (higher in HEB) of the increase in NOC abundance from clean days to polluted days in three cities with different energy consumption. In addition, the increased VC value (Table S1) on clean days (beneficial for the diffusion of pollutants) (Gani et al., 2019) was an important factor limiting the abundance of NOCs (Fig. 4), resulting in a lower NOC abundance on clean days compared to polluted days (Fig. 1).

As mentioned above, the aerosol NOCs of HZ were less affected by anthropogenic pollutants emitted from coal and natural gas combustion compared to HEB and BJ with cen-

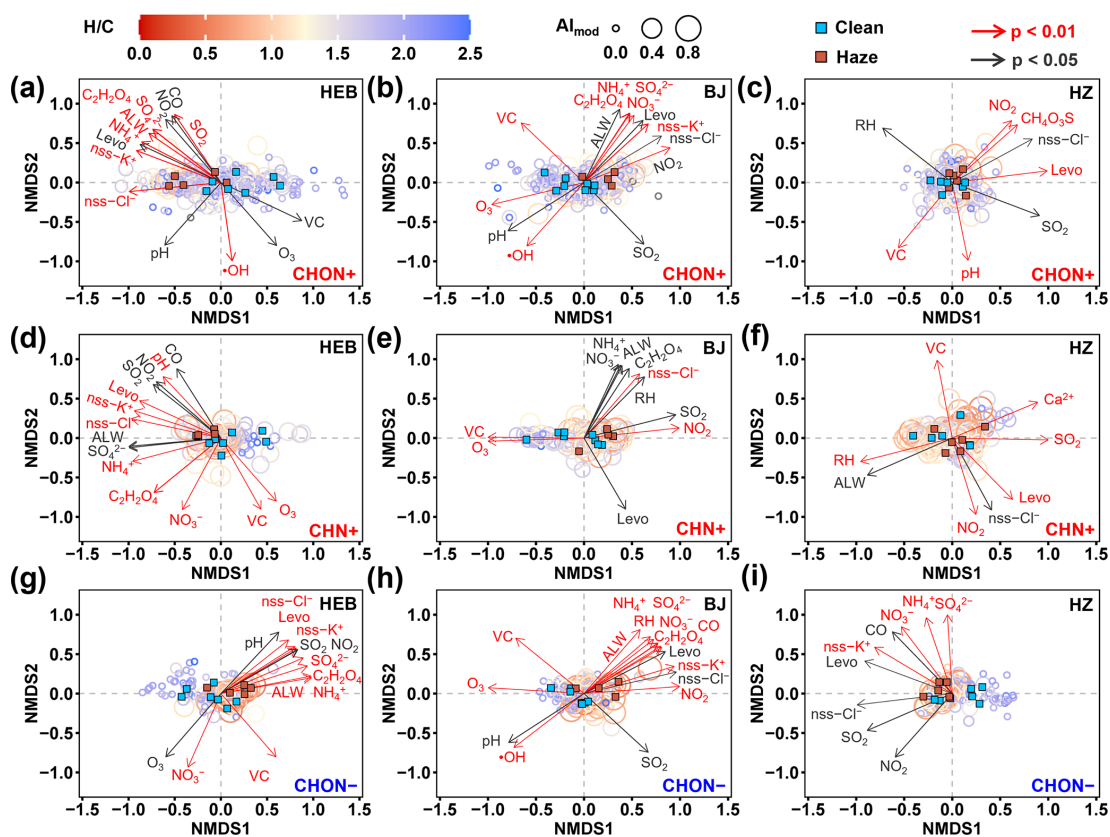


Figure 4. Non-metric multidimensional scaling of (a–c) CHON+, (d–f) CHN+, and (g–i) CHON– compounds from organic aerosol in different cities. The color and size of the circle indicate the H/C ratio and Al_{mod} value of compounds, respectively. Significant relationships between the variables and ordination (999 permutations) are indicated by $p < 0.05$ (gray) and $p < 0.01$ (red). Insignificant correlations are not shown. The scores of the samples collected during clean and haze periods are shown as blue and brown squares, respectively.

tralized heating. Interestingly, we found that the molecular distributions of most aromatic CHON+ compounds in HZ were influenced not only by some anthropogenic pollutants (e.g., SO_2 and NO_2) but also by methanesulfonic acid (CH_4O_3S) (Fig. 4c). Moreover, neither CHN+ nor CHON+ exhibited significant correlations with factors related to secondary processes in HZ (Fig. 4c and f). Methanesulfonic acid has been suggested to be a tracer for ocean aerosols (Ayers and Gras, 1991; Suess et al., 2019). These results suggest that aerosol CHON+ compounds in HZ may be influenced by long-distance-transport air masses originating from the ocean. This consideration can also be supported by the fact that only HZ was affected by air masses originating from the ocean (Fig. S13). Thus, marine emissions may be an important contributor to aerosol NOCs in HZ, which was significantly different from the cases of HEB and BJ where aromatic pollutants from fossil fuel combustion and aqueous-phase processes control the composition and abundance of aerosol NOCs.

3.4 Potential formation mechanisms of aerosol NOCs in cities with different energy consumption

Figure 5 shows the average signal intensity percentage and signal intensity distributions of NOCs formed by different aqueous-phase processes (Table S4 and Figs. S3–S5) in different cities during winter. The identification of specific reaction pathways is detailed in Figs. S3–S5 and Sect. S4. During the entire study period, the $cond_N$, $cond_hy_N$, and $cond_de_N$ pathways together accounted for more than 68 % (68 %–74 %) of the total signal intensity of CHON+ compounds in the three cities (Fig. 5a–c and Table S11). Specifically, the formation of CHON+ compounds was mainly dominated by the $cond_N$ and $cond_hy_N$ pathways in HEB, with less impact from the $cond_de_N$ pathway (Fig. 5a). However, CHON+ compounds derived from the $cond_de_N$ pathway showed a much higher proportion in BJ and HZ than in HEB (Fig. 5b and c). The $cond_de_N$ pathway involves both condensation and dehydration processes (Table S4 and Fig. S3). Recent studies have identified that dehydration reactions may occur in aerosols and fog water (Sun et al., 2024), as well as in photochemical transformations of organic compounds in the aqueous phase (Lian et

al., 2020). While the exact pathways of dehydration reactions in the particle phase remain uncertain, stronger solar radiation in BJ and HZ than in HEB (Table S1) may partly explain the higher signal proportion of CHON+ compounds formed through the cond_hy_N pathway in BJ and HZ. Furthermore, the higher signal proportions of CHN+ compounds formed through the de_N pathway in BJ (6 %) and HZ (11 %) than in HEB (2 %) may also be associated with this solar-radiation-induced dehydration mechanism (Fig. 5d–f and Table S12). For CHN+ compounds, the cond_de_N process dominated their formation (Fig. 5d–f). In general, the cond_N, cond_hy_N, and cond_de_N processes contributed most significantly to the formation of Re-NOCs in HEB, followed by BJ and HZ.

A typical mechanism for Re-NOC formation is the aqueous-phase reactions between carbonyl compounds and NH_4^+ (or NH_3) (Abudumutailifu et al., 2024; Laskin et al., 2014; Li et al., 2019b; Liu et al., 2023b; Wang et al., 2024). If this mechanism is simplified as a second-order reaction (i.e., [precursor] + [NH_3 and NH_4^+] \leftrightarrow [Re-NOCs]), the production of Re-NOCs is expected to be proportional to the abundances of precursors and NH_4^+ (Yang et al., 2023; Lin et al., 2023). Indeed, the signal intensities of the Re-CHON+ and Re-CHN+ compounds were significantly positively correlated with the signal intensities of their CHO precursors (identified using the precursor–product pairs theory; Figs. S3 and S4) and NH_4^+ concentrations in HEB (Fig. 6a, b, d, and e). This correlation gradually weakened from BJ to HZ (Fig. 6a, b, d, and e). As previously discussed, differences in energy consumption patterns resulted in the highest levels of anthropogenic aromatic compound emissions in HEB during the winter, followed by BJ, with the lowest levels in HZ (Figs. 2 and S14). Thus, the signal intensities of CHON+ and CHN+ compounds from cond_N, cond_de_N, and cond_hy_N processes were higher in HEB than in BJ and lowest in HZ (Fig. 5j and k).

Additionally, we noticed that the contribution of these aqueous-phase processes to the formation of CHON+ and CHN+ compounds increased significantly from clean to hazy days in HEB and BJ (Fig. 5). The increased ALW concentrations (Table S1) and atmospheric stability during haze periods likely provided favorable conditions for the precursors to undergo these aqueous-phase reactions, resulting in the formation of NOCs. Clearly, high pollutant emission levels in HEB provided a greater potential to convert precursors into more NOCs via the cond_N, cond_hy_N, and cond_de_N processes during haze periods. Thus, the hazy days in the HEB showed the largest increase in CHON+ and CHN+ compounds from the cond_N, cond_hy_N, and cond_de_N processes (Fig. 5j and k). In contrast, due to the absence of heating for generally mild winters and the implementation of stricter pollution control measures (more coal usage in HZ than in BJ, as shown in Fig. 1d), the precursor emissions in HZ were lower. These emissions were insufficient to support the production of large amounts of NOCs in

the aqueous phase. These results also indicate that emission reduction is the key to controlling aerosol NOC pollution.

CHON– compounds derived from the ox_hy_N and ox_N processes together accounted for more than 64 % (64 %–71 %) of the total signal intensity of CHON– compounds in the three cities (Fig. 5g–i, l and Table S13). The signal intensity proportions of CHON– compounds formed by the ox_hy_N process in these three cities (ranging from 47 % in HZ to 69 % in HEB) were higher than those in Wangdu (< 20 %) (Jiang et al., 2023). The observation study in Wangdu examined aerosol organic components only in ESI– mode (Jiang et al., 2023), which may underestimate the importance of the CHO+ compounds that could serve as precursors of Ox-NOCs. In general, CHON– compounds formed through the ox_hy_N and ox_N processes showed the highest abundance in HEB, followed by BJ and HZ (Fig. 5g–i). According to a simplified reaction mechanism for the formation of Ox-NOCs via aqueous-phase processes (i.e., [precursor] + [oxidants] \leftrightarrow [Ox-NOCs]) (Shi et al., 2023; Kroflič et al., 2015; Vione et al., 2005), we can infer that Ox-NOC production is proportional to precursor levels when oxidants (e.g., NO_2 radical or NO_2^+) are in a steady state in the atmosphere. Indeed, the signal intensities of the Ox-CHON– compounds were significantly positively correlated with the signal intensities of their CHO precursors identified using the precursor–product pair theory in HEB (Fig. 6c). Moreover, this correlation gradually weakened from BJ to HZ (Fig. 6c). Thus, the spatial differences in the contribution of the ox_hy_N and ox_N processes to Ox-NOC production across the three cities can also be explained by differences in precursor emission intensity, as indicated by the abovementioned Re-NOC formation.

4 Conclusion

The abundance, composition, potential precursors, and potential formation mechanisms of NOCs in $\text{PM}_{2.5}$ in three Chinese cities with different energy consumption types during the winter were systematically investigated. On average, the total signal intensity of NOCs (i.e., CHN+, CHON+, and CHON– compounds) was highest in HEB, followed by BJ. The lowest total NOC signal intensity was found in HZ. According to the identification of potential precursors of NOCs, we found that anthropogenic aromatic compounds were the main precursors of NOCs during winter in HEB, which mainly relies on coal for winter heating, with less impact from BVOCs. Anthropogenic aromatic precursors were also identified to be important contributors to NOC formation in BJ, which uses natural gas and coal for winter heating, although the contribution ratio was lower in BJ than in HEB. In contrast, due to generally mild winters resulting in the absence of a winter heating policy and the implementation of strict pollution control measures, as mentioned previously, aromatic precursor emissions in HZ were expected

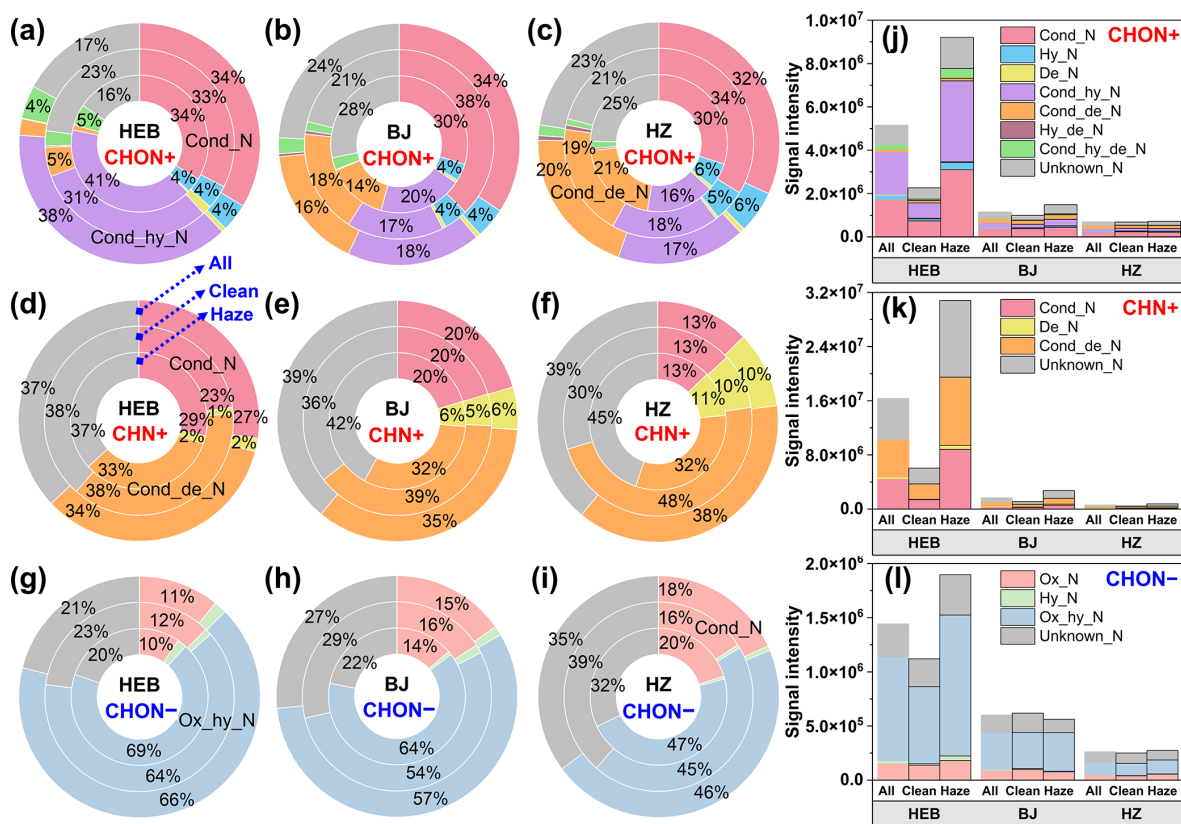


Figure 5. Average percentage distributions of signal intensities for aerosol (a–c) CHON+, (d–f) CHN+, and (g–i) CHON– compounds from various reaction pathways in different cities during winter. Average signal intensity distributions for aerosol (j) CHON+, (k) CHN+, and (l) CHON– compounds from various reaction pathways in different cities during winter.

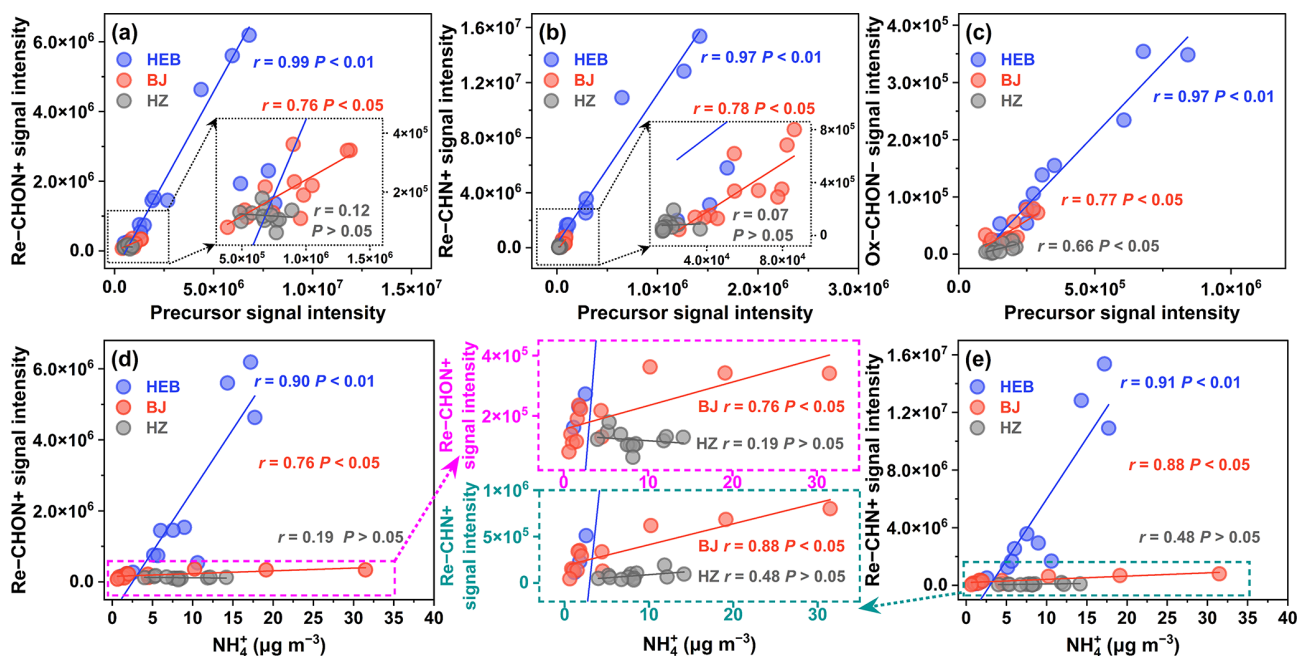


Figure 6. Signal intensity of (a) Re-CHON+, (b) Re-CHN+, and (c) Ox-CHON– compounds as functions of signal intensity of precursors (CHO compounds). Signal intensity of (d) Re-CHON+ and (e) Re-CHN+ compounds as functions of the concentrations of NH_4^+ .

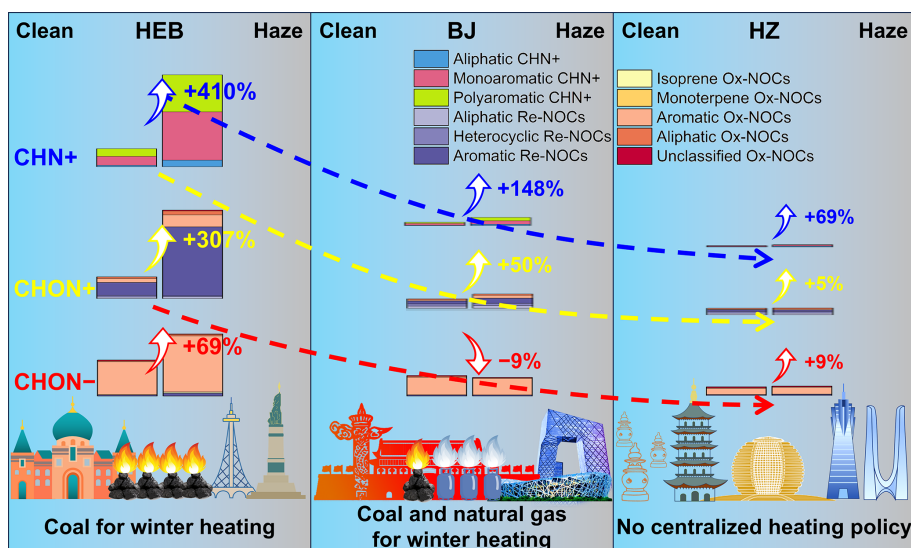


Figure 7. Conceptual illustration showing the characteristics of different NOCs from the clean days to the haze days in different cities.

to be the lowest. Furthermore, the NMDS analysis supported the fact that the impact of anthropogenic fossil fuel combustion on NOC pollution gradually decreased from HEB to BJ and then to HZ.

The formation of CHON+ compounds was mainly associated with the cond_N , cond_{hy}_N , and cond_{de}_N processes. The cond_N and cond_{de}_N processes dominated the formation of CHN+ compounds. The production of CHON+ and CHN+ compounds from the cond_N , cond_{hy}_N , and cond_{de}_N processes was highest in HEB, followed by BJ and HZ. The ox_{hy}_N and ox_N processes contributed significantly to the CHON– compound formation, from which the highest CHON– production occurred in HEB and the lowest in HZ. The spatial differences in the contribution of different aqueous-phase processes to NOC production in the three different cities can be attributed to differences in precursor emission intensity. In particular, the contribution of these aqueous-phase processes to the formation of CHON+ and CHN+ compounds showed the most significant increase from clean to hazy days in HEB, followed by BJ. We concluded that high pollutant emission levels can provide a greater potential to convert precursors to produce more NOCs via aqueous-phase processes during haze periods. The above findings are summarized in a diagram (Fig. 7).

In general, the aerosol NOC pollution during winter is closely linked to both the intensity of precursor emissions and the efficiency of aqueous-phase processes in converting these emissions into NOCs. The overall results highlight the importance of emission reduction strategies in controlling aerosol NOC pollution during winter. It is imperative to manage precursor emissions during hazy episodes in order to restrict the increased formation of secondary NOCs in conditions of high humidity. Moreover, targeted reduction of precursor emissions, especially from coal combus-

tion, could significantly mitigate NOC levels, thereby improving air quality and public health in urban areas. The transition to cleaner energy sources, as evidenced by the decreased gradient of NOC pollution from HEB to BJ to HZ, represents an effective pathway for the mitigation of NOC pollution. Future research should focus on further elucidating the specific pathways of aqueous-phase NOC formation and developing available models to predict NOC dynamics under varying environmental conditions. Additionally, research into the long-term effects of transitioning to cleaner energy sources on the reduction of NOC pollution will be essential for guiding effective air quality management strategies.

Code and data availability. The data presented in this work are available upon request from the corresponding authors. The code used in this study is available as part of the Vegan: Community Ecology Package (Oksanen, 2010) and can be accessed at CRAN: <https://doi.org/10.32614/CRAN.package.vegan>.

Supplement. The supplement related to this article is available online at <https://doi.org/10.5194/acp-25-2763-2025-supplement>.

Author contributions. YX designed the study. YJM, TY, LG, HX, and HWX performed field measurements and sample collection. YJM performed chemical analysis. YX and YJM performed data analysis. YX and YJM wrote the original manuscript. YX, YJM, and HYG reviewed and edited the manuscript.

Competing interests. The contact author has declared that none of the authors has any competing interests.

Disclaimer. Publisher's note: Copernicus Publications remains neutral with regard to jurisdictional claims made in the text, published maps, institutional affiliations, or any other geographical representation in this paper. While Copernicus Publications makes every effort to include appropriate place names, the final responsibility lies with the authors.

Acknowledgements. The authors are very grateful to the editor and the anonymous referees for their kind and valuable comments, which improved the paper.

Financial support. This research has been supported by the National Natural Science Foundation of China (grant no. 42303081), the Shanghai Science and Technology Innovation Action Plan of the Shanghai Sailing Program (grant no. 22YF1418700), and the National Key Research and Development Program of China (grant no. 2023YFF0806001).

Review statement. This paper was edited by Quanfu He and reviewed by four anonymous referees.

References

- Abudumutailifu, M., Shang, X., Wang, L., Zhang, M., Kang, H., Chen, Y., Li, L., Ju, R., Li, B., Ouyang, H., Tang, X., Li, C., Wang, L., Wang, X., George, C., Rudich, Y., Zhang, R., and Chen, J.: Unveiling the Molecular Characteristics, Origins, and Formation Mechanism of Reduced Nitrogen Organic Compounds in the Urban Atmosphere of Shanghai Using a Versatile Aerosol Concentration Enrichment System, *Environ. Sci. Technol.*, 58, 7099–7112, <https://doi.org/10.1021/acs.est.3c04071>, 2024.
- Arimoto, R., Duce, R. A., Savoie, D. L., Prospero, J. M., Talbot, R., Cullen, J. D., Tomza, U., Lewis, N. F., and Ray, B. J.: Relationships among aerosol constituents from Asia and the North Pacific during PEM-West A, *J. Geophys. Res.-Atmos.*, 101, 2011–2023, <https://doi.org/10.1029/95JD01071>, 1996.
- Ayers, G. P. and Gras, J. L.: Seasonal relationship between cloud condensation nuclei and aerosol methanesulphonate in marine air, *Nature*, 353, 834–835, <https://doi.org/10.1038/353834a0>, 1991.
- Bond, T. C., Wehner, B., Plewka, A., Wiedensohler, A., Heintzenberg, J., and Charlson, R. J.: Climate-relevant properties of primary particulate emissions from oil and natural gas combustion, *Atmos. Environ.*, 40, 3574–3587, <https://doi.org/10.1016/j.atmosenv.2005.12.030>, 2006.
- Cape, J. N., Cornell, S. E., Jickells, T. D., and Nemitz, E.: Organic nitrogen in the atmosphere – Where does it come from? A review of sources and methods, *Atmos. Res.*, 102, 30–48, <https://doi.org/10.1016/j.atmosres.2011.07.009>, 2011.
- Chao, A., Chazdon, R. L., Colwell, R. K., and Shen, T.-J.: Abundance-Based Similarity Indices and Their Estimation When There Are Unseen Species in Samples, *Biometrics*, 62, 361–371, <https://doi.org/10.1111/j.1541-0420.2005.00489.x>, 2006.
- Chen, Y., Guo, H., Nah, T., Tanner, D. J., Sullivan, A. P., Takeuchi, M., Gao, Z., Vasilakos, P., Russell, A. G., Baumann, K., Huey, L. G., Weber, R. J., and Ng, N. L.: Low-Molecular-Weight Carboxylic Acids in the Southeastern U.S.: Formation, Partitioning, and Implications for Organic Aerosol Aging, *Environ. Sci. Technol.*, 55, 6688–6699, <https://doi.org/10.1021/acs.est.1c01413>, 2021.
- Chen, Z. M., Wang, H. L., Zhu, L. H., Wang, C. X., Jie, C. Y., and Hua, W.: Aqueous-phase ozonolysis of methacrolein and methyl vinyl ketone: a potentially important source of atmospheric aqueous oxidants, *Atmos. Chem. Phys.*, 8, 2255–2265, <https://doi.org/10.5194/acp-8-2255-2008>, 2008.
- Ditto, J. C., Machesky, J., and Gentner, D. R.: Analysis of reduced and oxidized nitrogen-containing organic compounds at a coastal site in summer and winter, *Atmos. Chem. Phys.*, 22, 3045–3065, <https://doi.org/10.5194/acp-22-3045-2022>, 2022.
- Dong, P., Chen, Z., Qin, X., and Gong, Y.: Water Significantly Changes the Ring-Cleavage Process During Aqueous Photooxidation of Toluene, *Environ. Sci. Technol.*, 55, 16316–16325, <https://doi.org/10.1021/acs.est.1c04770>, 2021.
- Ehhalt, D. H. and Rohrer, F.: Dependence of the OH concentration on solar UV, *J. Geophys. Res.-Atmos.*, 105, 3565–3571, <https://doi.org/10.1029/1999JD901070>, 2000.
- Gani, S., Bhandari, S., Seraj, S., Wang, D. S., Patel, K., Soni, P., Arub, Z., Habib, G., Hildebrandt Ruiz, L., and Apte, J. S.: Sub-micron aerosol composition in the world's most polluted megacity: the Delhi Aerosol Supersite study, *Atmos. Chem. Phys.*, 19, 6843–6859, <https://doi.org/10.5194/acp-19-6843-2019>, 2019.
- Gao, J., Li, Y., Li, J., Shi, G., Liu, Z., Han, B., Tian, X., Wang, Y., Feng, Y., and Russell, A. G.: Impact of Formation Pathways on Secondary Inorganic Aerosol During Haze Pollution in Beijing: Quantitative Evidence From High-Resolution Observation and Modeling, *Geophys. Res. Lett.*, 48, e2021GL095623, <https://doi.org/10.1029/2021GL095623>, 2021.
- Gui, L., Xu, Y., You, Y.-C., Ma, Y.-J., Yang, T., Liu, T., Xiao, H.-W., Xiao, H., and Xiao, H.-Y.: Oxidative Degradation of Higher-Molecular-Weight Aromatic Amine Compounds Is a Potential Source of Anilinium in Urban Aerosols, *Environ. Sci. Technol. Lett.*, 11, 1355–1361, <https://doi.org/10.1021/acs.estlett.4c00935>, 2024.
- Guo, S., Hu, M., Zamora, M. L., Peng, J., Shang, D., Zheng, J., Du, Z., Wu, Z., Shao, M., Zeng, L., Molina, M. J., and Zhang, R.: Elucidating severe urban haze formation in China, *P. Natl. Acad. Sci. USA*, 111, 17373–17378, <https://doi.org/10.1073/pnas.1419604111>, 2014.
- Guo, Y., Yan, C., Liu, Y., Qiao, X., Zheng, F., Zhang, Y., Zhou, Y., Li, C., Fan, X., Lin, Z., Feng, Z., Zhang, Y., Zheng, P., Tian, L., Nie, W., Wang, Z., Huang, D., Daellenbach, K. R., Yao, L., Dada, L., Bianchi, F., Jiang, J., Liu, Y., Kerminen, V.-M., and Kulmala, M.: Seasonal variation in oxygenated organic molecules in urban Beijing and their contribution to secondary organic aerosol, *Atmos. Chem. Phys.*, 22, 10077–10097, <https://doi.org/10.5194/acp-22-10077-2022>, 2022.
- Hallquist, M., Wenger, J. C., Baltensperger, U., Rudich, Y., Simpson, D., Claeys, M., Dommen, J., Donahue, N. M., George, C., Goldstein, A. H., Hamilton, J. F., Herrmann, H., Hoffmann, T., Iinuma, Y., Jang, M., Jenkin, M. E., Jimenez, J. L., Kiendler-Scharr, A., Maenhaut, W., McFiggans, G., Mentel, Th. F., Monod, A., Prévôt, A. S. H., Seinfeld, J. H., Surratt, J. D.,

- Szmigielski, R., and Wildt, J.: The formation, properties and impact of secondary organic aerosol: current and emerging issues, *Atmos. Chem. Phys.*, 9, 5155–5236, <https://doi.org/10.5194/acp-9-5155-2009>, 2009.
- Han, Y., Zhang, X., Li, L., Lin, Y., Zhu, C., Zhang, N., Wang, Q., and Cao, J.: Enhanced Production of Organosulfur Species during a Severe Winter Haze Episode in the Guanzhong Basin of Northwest China, *Environ. Sci. Technol.*, 57, 8708–8718, <https://doi.org/10.1021/acs.est.3c02914>, 2023.
- He, C., Che, H., Bao, Z., Liu, Y., Li, Q., Hu, M., Zhou, J., Zhang, S., Yao, X., Shi, Q., Chen, C., Han, Y., Meng, L., Long, X., Yang, F., and Chen, Y.: Evolution of nucleophilic high molecular-weight organic compounds in ambient aerosols: a case study, *Atmos. Chem. Phys.*, 24, 1627–1639, <https://doi.org/10.5194/acp-24-1627-2024>, 2024.
- He, Q.-F., Ding, X., Fu, X.-X., Zhang, Y.-Q., Wang, J.-Q., Liu, Y.-X., Tang, M.-J., Wang, X.-M., and Rudich, Y.: Secondary Organic Aerosol Formation From Isoprene Epoxides in the Pearl River Delta, South China: IEPOX- and HMML-Derived Tracers, *J. Geophys. Res.-Atmos.*, 123, 6999–7012, <https://doi.org/10.1029/2017JD028242>, 2018.
- Heald, C. L., Kroll, J. H., Jimenez, J. L., Docherty, K. S., DeCarlo, P. F., Aiken, A. C., Chen, Q., Martin, S. T., Farmer, D. K., and Artaxo, P.: A simplified description of the evolution of organic aerosol composition in the atmosphere, *Geophys. Res. Lett.*, 37, L08803, <https://doi.org/10.1029/2010GL042737>, 2010.
- Hodas, N., Sullivan, A. P., Skog, K., Keutsch, F. N., Collett Jr., J. L., Decesari, S., Facchini, M. C., Carlton, A. G., Laaksonen, A., and Turpin, B. J.: Aerosol Liquid Water Driven by Anthropogenic Nitrate: Implications for Lifetimes of Water-Soluble Organic Gases and Potential for Secondary Organic Aerosol Formation, *Environ. Sci. Technol.*, 48, 11127–11136, <https://doi.org/10.1021/es5025096>, 2014.
- Huang, D., Zhang, X., Chen, Z. M., Zhao, Y., and Shen, X. L.: The kinetics and mechanism of an aqueous phase isoprene reaction with hydroxyl radical, *Atmos. Chem. Phys.*, 11, 7399–7415, <https://doi.org/10.5194/acp-11-7399-2011>, 2011.
- Huang, S., Shen, Z., Yang, X., Bai, G., Zhang, L., Zeng, Y., Sun, J., Xu, H., Ho, S. S. H., Zhang, Y., and Cao, J.: Nitroaromatic compounds in six major Chinese cities: Influence of different formation mechanisms on light absorption properties, *Sci. Total Environ.*, 930, 172672, <https://doi.org/10.1016/j.scitotenv.2024.172672>, 2024.
- Jiang, H., Li, J., Tang, J., Zhao, S., Chen, Y., Tian, C., Zhang, X., Jiang, B., Liao, Y., and Zhang, G.: Factors Influencing the Molecular Compositions and Distributions of Atmospheric Nitrogen-Containing Compounds, *J. Geophys. Res.-Atmos.*, 127, e2021JD036284, <https://doi.org/10.1029/2021JD036284>, 2022.
- Jiang, H., Cai, J., Feng, X., Chen, Y., Wang, L., Jiang, B., Liao, Y., Li, J., Zhang, G., Mu, Y., and Chen, J.: Aqueous-Phase Reactions of Anthropogenic Emissions Lead to the High Chemodiversity of Atmospheric Nitrogen-Containing Compounds during the Haze Event, *Environ. Sci. Technol.*, 57, 16500–16511, <https://doi.org/10.1021/acs.est.3c06648>, 2023.
- Jimenez, N. G., Sharp, K. D., Gramyk, T., Uglund, D. Z., Tran, M.-K., Rojas, A., Raffla, M. A., Stewart, D., Galloway, M. M., Lin, P., Laskin, A., Cazaunau, M., Pangui, E., Doussin, J.-F., and De Haan, D. O.: Radical-Initiated Brown Carbon Formation in Sunlit Carbonyl–Amine–Ammonium Sulfate Mixtures and Aqueous Aerosol Particles, *ACS Earth Space Chem.*, 6, 228–238, <https://doi.org/10.1021/acsearthspacechem.1c00395>, 2022.
- Kellerman, A. M., Dittmar, T., Kothawala, D. N., and Tranvik, L. J.: Chemodiversity of dissolved organic matter in lakes driven by climate and hydrology, *Nat. Commun.*, 5, 3804, <https://doi.org/10.1038/ncomms4804>, 2014.
- Koch, B. P. and Dittmar, T.: From mass to structure: an aromaticity index for high-resolution mass data of natural organic matter, *Rapid Commun. Mass Spectrom.*, 20, 926–932, <https://doi.org/10.1002/rcm.2386>, 2006.
- Krofič, A., Grilc, M., and Grčić, I.: Does toxicity of aromatic pollutants increase under remote atmospheric conditions?, *Sci. Rep.*, 5, 8859, <https://doi.org/10.1038/srep08859>, 2015.
- Kroll, J. H., Donahue, N. M., Jimenez, J. L., Kessler, S. H., Canagaratna, M. R., Wilson, K. R., Altieri, K. E., Mazzoleni, L. R., Wozniak, A. S., Bluhm, H., Mysak, E. R., Smith, J. D., Kolb, C. E., and Worsnop, D. R.: Carbon oxidation state as a metric for describing the chemistry of atmospheric organic aerosol, *Nat. Chem.*, 3, 133–139, <https://doi.org/10.1038/nchem.948>, 2011.
- Křůmal, K., Mikuška, P., Horák, J., Hopan, F., and Krpec, K.: Comparison of emissions of gaseous and particulate pollutants from the combustion of biomass and coal in modern and old-type boilers used for residential heating in the Czech Republic, Central Europe, *Chemosphere*, 229, 51–59, <https://doi.org/10.1016/j.chemosphere.2019.04.137>, 2019.
- Kuwata, M. and Martin, S. T.: Phase of atmospheric secondary organic material affects its reactivity, *P. Natl. Acad. Sci. USA*, 109, 17354–17359, <https://doi.org/10.1073/pnas.1209071109>, 2012.
- Laskin, J., Laskin, A., Nizkorodov, S. A., Roach, P., Eckert, P., Gilles, M. K., Wang, B., Lee, H. J., and Hu, Q.: Molecular Selectivity of Brown Carbon Chromophores, *Environ. Sci. Technol.*, 48, 12047–12055, <https://doi.org/10.1021/es503432r>, 2014.
- Lee, A. K. Y., Zhao, R., Li, R., Liggio, J., Li, S.-M., and Abbatt, J. P. D.: Formation of Light Absorbing Organo-Nitrogen Species from Evaporation of Droplets Containing Glyoxal and Ammonium Sulfate, *Environ. Sci. Technol.*, 47, 12819–12826, <https://doi.org/10.1021/es402687w>, 2013.
- Li, X., Song, S., Zhou, W., Hao, J., Worsnop, D. R., and Jiang, J.: Interactions between aerosol organic components and liquid water content during haze episodes in Beijing, *Atmos. Chem. Phys.*, 19, 12163–12174, <https://doi.org/10.5194/acp-19-12163-2019>, 2019a.
- Li, Y., Fu, T.-M., Yu, J. Z., Yu, X., Chen, Q., Miao, R., Zhou, Y., Zhang, A., Ye, J., Yang, X., Tao, S., Liu, H., and Yao, W.: Dissecting the contributions of organic nitrogen aerosols to global atmospheric nitrogen deposition and implications for ecosystems, *Natl. Sci. Rev.*, 10, nwad244, <https://doi.org/10.1093/nsr/nwad244>, 2023.
- Li, Z., Nizkorodov, S. A., Chen, H., Lu, X., Yang, X., and Chen, J.: Nitrogen-containing secondary organic aerosol formation by acrolein reaction with ammonia/ammonium, *Atmos. Chem. Phys.*, 19, 1343–1356, <https://doi.org/10.5194/acp-19-1343-2019>, 2019b.
- Lian, L., Yan, S., Zhou, H., and Song, W.: Overview of the Phototransformation of Wastewater Effluents by High-Resolution Mass Spectrometry, *Environ. Sci. Technol.*, 54, 1816–1826, <https://doi.org/10.1021/acs.est.9b04669>, 2020.

- Lin, X., Xu, Y., Zhu, R.-G., Xiao, H.-W., and Xiao, H.-Y.: Proteinaceous Matter in PM_{2.5} in Suburban Guiyang, Southwestern China: Decreased Importance in Long-Range Transport and Atmospheric Degradation, *J. Geophys. Res.-Atmos.*, 128, e2023JD038516, <https://doi.org/10.1029/2023JD038516>, 2023.
- Liu, T., Xu, Y., Sun, Q.-B., Xiao, H.-W., Zhu, R.-G., Li, C.-X., Li, Z.-Y., Zhang, K.-Q., Sun, C.-X., and Xiao, H.-Y.: Characteristics, Origins, and Atmospheric Processes of Amines in Fine Aerosol Particles in Winter in China, *J. Geophys. Res.-Atmos.*, 128, e2023JD038974, <https://doi.org/10.1029/2023JD038974>, 2023a.
- Liu, X., Wang, H., Wang, F., Lv, S., Wu, C., Zhao, Y., Zhang, S., Liu, S., Xu, X., Lei, Y., and Wang, G.: Secondary Formation of Atmospheric Brown Carbon in China Haze: Implication for an Enhancing Role of Ammonia, *Environ. Sci. Technol.*, 57, 11163–11172, <https://doi.org/10.1021/acs.est.3c03948>, 2023b.
- Liu, X.-Y., He, K.-B., Zhang, Q., Lu, Z.-F., Wang, S.-W., Zhang, Y.-X., and Streets, D. G.: Analysis of the origins of black carbon and carbon monoxide transported to Beijing, Tianjin, and Hebei in China, *Sci. Total Environ.*, 653, 1364–1376, <https://doi.org/10.1016/j.scitotenv.2018.09.274>, 2019.
- Liu, Y., Nie, W., Li, Y., Ge, D., Liu, C., Xu, Z., Chen, L., Wang, T., Wang, L., Sun, P., Qi, X., Wang, J., Xu, Z., Yuan, J., Yan, C., Zhang, Y., Huang, D., Wang, Z., Donahue, N. M., Worsnop, D., Chi, X., Ehn, M., and Ding, A.: Formation of condensable organic vapors from anthropogenic and biogenic volatile organic compounds (VOCs) is strongly perturbed by NO_x in eastern China, *Atmos. Chem. Phys.*, 21, 14789–14814, <https://doi.org/10.5194/acp-21-14789-2021>, 2021.
- Liu, Z., Zhu, B., Zhu, C., Ruan, T., Li, J., Chen, H., Li, Q., Wang, X., Wang, L., Mu, Y., Collett, J., George, C., Wang, Y., Wang, X., Su, J., Yu, S., Mellouki, A., Chen, J., and Jiang, G.: Abundant nitrogenous secondary organic aerosol formation accelerated by cloud processing, *iScience*, 26, 108317, <https://doi.org/10.1016/j.isci.2023.108317>, 2023c.
- Lv, S., Wang, F., Wu, C., Chen, Y., Liu, S., Zhang, S., Li, D., Du, W., Zhang, F., Wang, H., Huang, C., Fu, Q., Duan, Y., and Wang, G.: Gas-to-Aerosol Phase Partitioning of Atmospheric Water-Soluble Organic Compounds at a Rural Site in China: An Enhancing Effect of NH₃ on SOA Formation, *Environ. Sci. Technol.*, 56, 3915–3924, <https://doi.org/10.1021/acs.est.1c06855>, 2022.
- Ma, L., Li, B., Liu, Y., Sun, X., Fu, D., Sun, S., Thapa, S., Geng, J., Qi, H., Zhang, A., and Tian, C.: Characterization, sources and risk assessment of PM_{2.5}-bound polycyclic aromatic hydrocarbons (PAHs) and nitrated PAHs (NPAHs) in Harbin, a cold city in Northern China, *J. Clean. Prod.*, 264, 121673, <https://doi.org/10.1016/j.jclepro.2020.121673>, 2020.
- Ma, Y.-J., Xu, Y., Yang, T., Xiao, H.-W., and Xiao, H.-Y.: Measurement report: Characteristics of nitrogen-containing organics in PM_{2.5} in Ürümqi, northwestern China – differential impacts of combustion of fresh and aged biomass materials, *Atmos. Chem. Phys.*, 24, 4331–4346, <https://doi.org/10.5194/acp-24-4331-2024>, 2024.
- Mafusire, G., Annegarn, H. J., Vakkari, V., Beukes, J. P., Josipovic, M., van Zyl, P. G., and Laakso, L.: Submicrometer aerosols and excess CO as tracers for biomass burning air mass transport over southern Africa, *J. Geophys. Res.-Atmos.*, 121, 10262–10282, <https://doi.org/10.1002/2015JD023965>, 2016.
- MEEPRC: Technical Regulation on Ambient Air Quality Index (on trial): HJ 633–2012, Ministry of Ecology and Environment of the People's Republic of China, https://www.mee.gov.cn/ywgz/fgbz/bz/bzwb/jcffbz/201203/t20120302_224166.shtml (last access: 10 December 2024), 2012.
- Montoya-Aguilera, J., Hinks, M. L., Aiona, P. K., Wingen, L. M., Horne, J. R., Zhu, S., Dabdub, D., Laskin, A., Laskin, J., Lin, P., and Nizkorodov, S. A.: Reactive Uptake of Ammonia by Biogenic and Anthropogenic Organic Aerosols, in: *Multiphase Environmental Chemistry in the Atmosphere*, edited by: Hunt, S. W., Laskin, A., and Nizkorodov, S. A., American Chemical Society, Washington, DC, 127–147, <https://doi.org/10.1021/bk-2018-1299.ch007>, 2018.
- Ng, N. L., Brown, S. S., Archibald, A. T., Atlas, E., Cohen, R. C., Crowley, J. N., Day, D. A., Donahue, N. M., Fry, J. L., Fuchs, H., Griffin, R. J., Guzman, M. I., Herrmann, H., Hodzic, A., Iinuma, Y., Jimenez, J. L., Kiendler-Scharr, A., Lee, B. H., Luecken, D. J., Mao, J., McLaren, R., Mutzel, A., Osthoff, H. D., Ouyang, B., Picquet-Varrault, B., Platt, U., Pye, H. O. T., Rudich, Y., Schwantes, R. H., Shiraiwa, M., Stutz, J., Thornton, J. A., Tilgner, A., Williams, B. J., and Zaveri, R. A.: Nitrate radicals and biogenic volatile organic compounds: oxidation, mechanisms, and organic aerosol, *Atmos. Chem. Phys.*, 17, 2103–2162, <https://doi.org/10.5194/acp-17-2103-2017>, 2017.
- Nguyen, T. B., Bates, K. H., Crouse, J. D., Schwantes, R. H., Zhang, X., Kjaergaard, H. G., Surratt, J. D., Lin, P., Laskin, A., Seinfeld, J. H., and Wennberg, P. O.: Mechanism of the hydroxyl radical oxidation of methacryloyl peroxyxynitrate (MPAN) and its pathway toward secondary organic aerosol formation in the atmosphere, *Phys. Chem. Chem. Phys.*, 17, 17914–17926, <https://doi.org/10.1039/C5CP02001H>, 2015.
- Nie, W., Yan, C., Huang, D. D., Wang, Z., Liu, Y., Qiao, X., Guo, Y., Tian, L., Zheng, P., Xu, Z., Li, Y., Xu, Z., Qi, X., Sun, P., Wang, J., Zheng, F., Li, X., Yin, R., Dallenbach, K. R., Bianchi, F., Petäjä, T., Zhang, Y., Wang, M., Schervish, M., Wang, S., Qiao, L., Wang, Q., Zhou, M., Wang, H., Yu, C., Yao, D., Guo, H., Ye, P., Lee, S., Li, Y. J., Liu, Y., Chi, X., Kerminen, V.-M., Ehn, M., Donahue, N. M., Wang, T., Huang, C., Kulmala, M., Worsnop, D., Jiang, J., and Ding, A.: Secondary organic aerosol formed by condensing anthropogenic vapours over China's megacities, *Nat. Geosci.*, 15, 255–261, <https://doi.org/10.1038/s41561-022-00922-5>, 2022.
- Nozière, B., Kalberer, M., Claeys, M., Allan, J., D'Anna, B., Decesari, S., Finessi, E., Glasius, M., Grgić, I., Hamilton, J. F., Hoffmann, T., Iinuma, Y., Jaoui, M., Kahnt, A., Kampf, C. J., Kourtschev, I., Maenhaut, W., Marsden, N., Saarikoski, S., Schnelle-Kreis, J., Surratt, J. D., Szidat, S., Szmigielski, R., and Wisthaler, A.: The Molecular Identification of Organic Compounds in the Atmosphere: State of the Art and Challenges, *Chem. Rev.*, 115, 3919–3983, <https://doi.org/10.1021/cr5003485>, 2015.
- Oksanen, J.: Vegan: Community Ecology Package, 2.6-8, CRAN [code], <https://doi.org/10.32614/CRAN.package.vegan>, 2010.
- Perraud, V., Bruns, E. A., Ezell, M. J., Johnson, S. N., Yu, Y., Alexander, M. L., Zelenyuk, A., Imre, D., Chang, W. L., Dabdub, D., Pankow, J. F., and Finlayson-Pitts, B. J.: Nonequilibrium atmospheric secondary organic aerosol formation and growth, *P. Natl. Acad. Sci. USA*, 109, 2836–2841, <https://doi.org/10.1073/pnas.1119909109>, 2012.

- Rollins, A. W., Browne, E. C., Min, K.-E., Pusede, S. E., Wooldridge, P. J., Gentner, D. R., Goldstein, A. H., Liu, S., Day, D. A., Russell, L. M., and Cohen, R. C.: Evidence for NO_x Control over Nighttime SOA Formation, *Science*, 337, 1210–1212, <https://doi.org/10.1126/science.1221520>, 2012.
- Shen, Z., Cao, J., Arimoto, R., Han, Z., Zhang, R., Han, Y., Liu, S., Okuda, T., Nakao, S., and Tanaka, S.: Ionic composition of TSP and PM_{2.5} during dust storms and air pollution episodes at Xi'an, China, *Atmos. Environ.*, 43, 2911–2918, <https://doi.org/10.1016/j.atmosenv.2009.03.005>, 2009.
- Shi, X., Qiu, X., Cheng, Z., Chen, Q., Rudich, Y., and Zhu, T.: Isomeric Identification of Particle-Phase Organic Nitrates through Gas Chromatography and Time-of-Flight Mass Spectrometry Coupled with an Electron Capture Negative Ionization Source, *Environ. Sci. Technol.*, 54, 707–713, <https://doi.org/10.1021/acs.est.9b05818>, 2020.
- Shi, X., Qiu, X., Li, A., Jiang, X., Wei, G., Zheng, Y., Chen, Q., Chen, S., Hu, M., Rudich, Y., and Zhu, T.: Polar Nitrated Aromatic Compounds in Urban Fine Particulate Matter: A Focus on Formation via an Aqueous-Phase Radical Mechanism, *Environ. Sci. Technol.*, 57, 5160–5168, <https://doi.org/10.1021/acs.est.2c07324>, 2023.
- Singh, S. and Kumar, R.: Air Pollution and Its Associated Impacts on Atmosphere and Biota Health, in: *Extremes in Atmospheric Processes and Phenomenon: Assessment, Impacts and Mitigation*, edited by: Saxena, P., Shukla, A., and Gupta, A. K., Springer Nature Singapore, Singapore, 29–58, https://doi.org/10.1007/978-981-16-7727-4_3, 2022.
- Song, J., Li, M., Jiang, B., Wei, S., Fan, X., and Peng, P. A.: Molecular Characterization of Water-Soluble Humic like Substances in Smoke Particles Emitted from Combustion of Biomass Materials and Coal Using Ultrahigh-Resolution Electrospray Ionization Fourier Transform Ion Cyclotron Resonance Mass Spectrometry, *Environ. Sci. Technol.*, 52, 2575–2585, <https://doi.org/10.1021/acs.est.7b06126>, 2018.
- Song, J., Li, M., Zou, C., Cao, T., Fan, X., Jiang, B., Yu, Z., Jia, W., and Peng, P. a.: Molecular Characterization of Nitrogen-Containing Compounds in Humic-like Substances Emitted from Biomass Burning and Coal Combustion, *Environ. Sci. Technol.*, 56, 119–130, <https://doi.org/10.1021/acs.est.1c04451>, 2022.
- Stockwell, C. E., Veres, P. R., Williams, J., and Yokelson, R. J.: Characterization of biomass burning emissions from cooking fires, peat, crop residue, and other fuels with high-resolution proton-transfer-reaction time-of-flight mass spectrometry, *Atmos. Chem. Phys.*, 15, 845–865, <https://doi.org/10.5194/acp-15-845-2015>, 2015.
- Streets, D. G. and Waldhoff, S. T.: Present and future emissions of air pollutants in China: SO₂, NO_x, and CO, *Atmos. Environ.*, 34, 363–374, [https://doi.org/10.1016/S1352-2310\(99\)00167-3](https://doi.org/10.1016/S1352-2310(99)00167-3), 2000.
- Su, S., Xie, Q., Lang, Y., Cao, D., Xu, Y., Chen, J., Chen, S., Hu, W., Qi, Y., Pan, X., Sun, Y., Wang, Z., Liu, C.-Q., Jiang, G., and Fu, P.: High Molecular Diversity of Organic Nitrogen in Urban Snow in North China, *Environ. Sci. Technol.*, 55, 4344–4356, <https://doi.org/10.1021/acs.est.0c06851>, 2021.
- Suess, E., Aemisegger, F., Sonke, J. E., Sprenger, M., Wernli, H., and Winkel, L. H. E.: Marine versus Continental Sources of Iodine and Selenium in Rainfall at Two European High-Altitude Locations, *Environ. Sci. Technol.*, 53, 1905–1917, <https://doi.org/10.1021/acs.est.8b05533>, 2019.
- Sun, W., Hu, X., Fu, Y., Zhang, G., Zhu, Y., Wang, X., Yan, C., Xue, L., Meng, H., Jiang, B., Liao, Y., Wang, X., Peng, P., and Bi, X.: Different formation pathways of nitrogen-containing organic compounds in aerosols and fog water in northern China, *Atmos. Chem. Phys.*, 24, 6987–6999, <https://doi.org/10.5194/acp-24-6987-2024>, 2024.
- Surratt, J. D., Chan, A. W. H., Eddingsaas, N. C., Chan, M., Loza, C. L., Kwan, A. J., Hersey, S. P., Flagan, R. C., Wennberg, P. O., and Seinfeld, J. H.: Reactive intermediates revealed in secondary organic aerosol formation from isoprene, *P. Natl. Acad. Sci. USA*, 107, 6640–6645, <https://doi.org/10.1073/pnas.0911114107>, 2010.
- Vione, D., Maurino, V., Minero, C., and Pelizzetti, E.: Aqueous Atmospheric Chemistry: Formation of 2,4-Dinitrophenol upon Nitration of 2-Nitrophenol and 4-Nitrophenol in Solution, *Environ. Sci. Technol.*, 39, 7921–7931, <https://doi.org/10.1021/es050824m>, 2005.
- Vu, T. V., Shi, Z., Cheng, J., Zhang, Q., He, K., Wang, S., and Harrison, R. M.: Assessing the impact of clean air action on air quality trends in Beijing using a machine learning technique, *Atmos. Chem. Phys.*, 19, 11303–11314, <https://doi.org/10.5194/acp-19-11303-2019>, 2019.
- Wang, D., Shen, Z., Yang, X., Huang, S., Luo, Y., Bai, G., and Cao, J.: Insight into the Role of NH₃/NH₄⁺ and NO_x/NO₃⁻ in the Formation of Nitrogen-Containing Brown Carbon in Chinese Megacities, *Environ. Sci. Technol.*, 58, 4281–4290, <https://doi.org/10.1021/acs.est.3c10374>, 2024.
- Wang, J., Sun, S., Zhang, C., Xue, C., Liu, P., Zhang, C., Mu, Y., Wu, H., Wang, D., Chen, H., and Chen, J.: The pollution levels, variation characteristics, sources and implications of atmospheric carbonyls in a typical rural area of North China Plain during winter, *J. Environ. Sci.*, 95, 256–265, <https://doi.org/10.1016/j.jes.2020.05.003>, 2020.
- Wang, J., Ye, J., Zhang, Q., Zhao, J., Wu, Y., Li, J., Liu, D., Li, W., Zhang, Y., Wu, C., Xie, C., Qin, Y., Lei, Y., Huang, X., Guo, J., Liu, P., Fu, P., Li, Y., Lee, H. C., Choi, H., Zhang, J., Liao, H., Chen, M., Sun, Y., Ge, X., Martin, S. T., and Jacob, D. J.: Aqueous production of secondary organic aerosol from fossil-fuel emissions in winter Beijing haze, *P. Natl. Acad. Sci. USA*, 118, e2022179118, <https://doi.org/10.1073/pnas.2022179118>, 2021a.
- Wang, K., Zhang, Y., Huang, R.-J., Cao, J., and Hoffmann, T.: UHPLC-Orbitrap mass spectrometric characterization of organic aerosol from a central European city (Mainz, Germany) and a Chinese megacity (Beijing), *Atmos. Environ.*, 189, 22–29, <https://doi.org/10.1016/j.atmosenv.2018.06.036>, 2018.
- Wang, K., Huang, R.-J., Brüggemann, M., Zhang, Y., Yang, L., Ni, H., Guo, J., Wang, M., Han, J., Bilde, M., Glasius, M., and Hoffmann, T.: Urban organic aerosol composition in eastern China differs from north to south: molecular insight from a liquid chromatography–mass spectrometry (Orbitrap) study, *Atmos. Chem. Phys.*, 21, 9089–9104, <https://doi.org/10.5194/acp-21-9089-2021>, 2021b.
- Wang, Y., Zhuang, G., Zhang, X., Huang, K., Xu, C., Tang, A., Chen, J., and An, Z.: The ion chemistry, seasonal cycle, and sources of PM_{2.5} and TSP aerosol in Shanghai, *Atmos. Environ.*, 40, 2935–2952, <https://doi.org/10.1016/j.atmosenv.2005.12.051>, 2006.

- Wang, Y., Hu, M., Lin, P., Guo, Q., Wu, Z., Li, M., Zeng, L., Song, Y., Zeng, L., Wu, Y., Guo, S., Huang, X., and He, L.: Molecular Characterization of Nitrogen-Containing Organic Compounds in Humic-like Substances Emitted from Straw Residue Burning, *Environ. Sci. Technol.*, 51, 5951–5961, <https://doi.org/10.1021/acs.est.7b00248>, 2017.
- Wang, Y., Zhao, Y., Li, Z., Li, C., Yan, N., and Xiao, H.: Importance of Hydroxyl Radical Chemistry in Isoprene Suppression of Particle Formation from α -Pinene Ozonolysis, *ACS Earth Space Chem.*, 5, 487–499, <https://doi.org/10.1021/acsearthspacechem.0c00294>, 2021c.
- Wang, Y., Hu, M., Hu, W., Zheng, J., Niu, H., Fang, X., Xu, N., Wu, Z., Guo, S., Wu, Y., Chen, W., Lu, S., Shao, M., Xie, S., Luo, B., and Zhang, Y.: Secondary Formation of Aerosols Under Typical High-Humidity Conditions in Wintertime Sichuan Basin, China: A Contrast to the North China Plain, *J. Geophys. Res.-Atmos.*, 126, e2021JD034560, <https://doi.org/10.1029/2021JD034560>, 2021d.
- Wen, W., Shi, L., Li, L., Wang, L., and Chen, J.: Molecular characteristics of ambient organic aerosols in Shanghai winter before and after the COVID-19 outbreak, *Sci. Total Environ.*, 869, 161811, <https://doi.org/10.1016/j.scitotenv.2023.161811>, 2023.
- Wu, Z., Wang, Y., Tan, T., Zhu, Y., Li, M., Shang, D., Wang, H., Lu, K., Guo, S., Zeng, L., and Zhang, Y.: Aerosol Liquid Water Driven by Anthropogenic Inorganic Salts: Implying Its Key Role in Haze Formation over the North China Plain, *Environ. Sci. Technol. Lett.*, 5, 160–166, <https://doi.org/10.1021/acs.estlett.8b00021>, 2018.
- Xi, Y., Wang, Q., Zhu, J., Yang, M., Hao, T., Chen, Y., Zhang, Q., He, N., and Yu, G.: Atmospheric wet organic nitrogen deposition in China: Insights from the national observation network, *Sci. Total Environ.*, 898, 165629, <https://doi.org/10.1016/j.scitotenv.2023.165629>, 2023.
- Xiao, H.-Y. and Liu, C.-Q.: Chemical characteristics of water-soluble components in TSP over Guiyang, SW China, 2003, *Atmos. Environ.*, 38, 6297–6306, <https://doi.org/10.1016/j.atmosenv.2004.08.033>, 2004.
- Xu, B., Zhang, G., Gustafsson, Ö., Kawamura, K., Li, J., Anderson, A., Bikkina, S., Kunwar, B., Pokhrel, A., Zhong, G., Zhao, S., Li, J., Huang, C., Cheng, Z., Zhu, S., Peng, P., and Sheng, G.: Large contribution of fossil-derived components to aqueous secondary organic aerosols in China, *Nat. Commun.*, 13, 5115, <https://doi.org/10.1038/s41467-022-32863-3>, 2022a.
- Xu, Y., Xiao, H., Wu, D., and Long, C.: Abiotic and Biological Degradation of Atmospheric Proteinaceous Matter Can Contribute Significantly to Dissolved Amino Acids in Wet Deposition, *Environ. Sci. Technol.*, 54, 6551–6561, <https://doi.org/10.1021/acs.est.0c00421>, 2020a.
- Xu, Y., Miyazaki, Y., Tachibana, E., Sato, K., Ramasamy, S., Mochizuki, T., Sadanaga, Y., Nakashima, Y., Sakamoto, Y., Matsuda, K., and Kajii, Y.: Aerosol Liquid Water Promotes the Formation of Water-Soluble Organic Nitrogen in Submicrometer Aerosols in a Suburban Forest, *Environ. Sci. Technol.*, 54, 1406–1414, <https://doi.org/10.1021/acs.est.9b05849>, 2020b.
- Xu, Y., Dong, X.-N., Xiao, H.-Y., He, C., and Wu, D.-S.: Water-Insoluble Components in Rainwater in Suburban Guiyang, Southwestern China: A Potential Contributor to Dissolved Organic Carbon, *J. Geophys. Res.-Atmos.*, 127, e2022JD037721, <https://doi.org/10.1029/2022JD037721>, 2022b.
- Xu, Y., Dong, X.-N., Xiao, H.-Y., Zhou, J.-X., and Wu, D.-S.: Proteinaceous Matter and Liquid Water in Fine Aerosols in Nanchang, Eastern China: Seasonal Variations, Sources, and Potential Connections, *J. Geophys. Res.-Atmos.*, 127, e2022JD036589, <https://doi.org/10.1029/2022JD036589>, 2022c.
- Xu, Y., Dong, X.-N., He, C., Wu, D.-S., Xiao, H.-W., and Xiao, H.-Y.: Mist cannon trucks can exacerbate the formation of water-soluble organic aerosol and PM_{2.5} pollution in the road environment, *Atmos. Chem. Phys.*, 23, 6775–6788, <https://doi.org/10.5194/acp-23-6775-2023>, 2023.
- Xu, Y., Lin, X., Sun, Q.-B., Xiao, H.-W., Xiao, H., and Xiao, H.-Y.: Elaborating the Atmospheric Transformation of Combined and Free Amino Acids From the Perspective of Observational Studies, *J. Geophys. Res.-Atmos.*, 129, e2024JD040730, <https://doi.org/10.1029/2024JD040730>, 2024a.
- Xu, Y., Liu, T., Ma, Y.-J., Sun, Q.-B., Xiao, H.-W., Xiao, H., Xiao, H.-Y., and Liu, C.-Q.: Measurement report: Occurrence of aminiums in PM_{2.5} during winter in China – aminium outbreak during polluted episodes and potential constraints, *Atmos. Chem. Phys.*, 24, 10531–10542, <https://doi.org/10.5194/acp-24-10531-2024>, 2024b.
- Yan, F., Su, H., Cheng, Y., Huang, R., Liao, H., Yang, T., Zhu, Y., Zhang, S., Sheng, L., Kou, W., Zeng, X., Xiang, S., Yao, X., Gao, H., and Gao, Y.: Frequent haze events associated with transport and stagnation over the corridor between the North China Plain and Yangtze River Delta, *Atmos. Chem. Phys.*, 24, 2365–2376, <https://doi.org/10.5194/acp-24-2365-2024>, 2024.
- Yang, L., Huang, R.-J., Yuan, W., Huang, D. D., and Huang, C.: pH-Dependent Aqueous-Phase Brown Carbon Formation: Rate Constants and Implications for Solar Absorption and Atmospheric Photochemistry, *Environ. Sci. Technol.*, 58, 1236–1243, <https://doi.org/10.1021/acs.est.3c07631>, 2024a.
- Yang, T., Xu, Y., Ye, Q., Ma, Y.-J., Wang, Y.-C., Yu, J.-Z., Duan, Y.-S., Li, C.-X., Xiao, H.-W., Li, Z.-Y., Zhao, Y., and Xiao, H.-Y.: Spatial and diurnal variations of aerosol organosulfates in summertime Shanghai, China: potential influence of photochemical processes and anthropogenic sulfate pollution, *Atmos. Chem. Phys.*, 23, 13433–13450, <https://doi.org/10.5194/acp-23-13433-2023>, 2023.
- Yang, T., Xu, Y., Ma, Y.-J., Wang, Y.-C., Yu, J. Z., Sun, Q.-B., Xiao, H.-W., Xiao, H.-Y., and Liu, C.-Q.: Field Evidence for Constraints of Nearly Dry and Weakly Acidic Aerosol Conditions on the Formation of Organosulfates, *Environ. Sci. Technol. Lett.*, 11, 981–987, <https://doi.org/10.1021/acs.estlett.4c00522>, 2024b.
- Yang, X., Huang, S., Li, D., Xu, H., Zeng, Y., Yang, L., Wang, D., Zhang, N., Cao, J., and Shen, Z.: Water-soluble organic matter with various polarities in PM_{2.5} over Xi'an, China: Abundance, functional groups, and light absorption, *Particuology*, 84, 281–289, <https://doi.org/10.1016/j.partic.2023.07.005>, 2024c.
- Yassine, M. M., Harir, M., Dabek-Zlotorzynska, E., and Schmitt-Kopplin, P.: Structural characterization of organic aerosol using Fourier transform ion cyclotron resonance mass spectrometry: Aromaticity equivalent approach, *Rapid Commun. Mass Spectrom.*, 28, 2445–2454, <https://doi.org/10.1002/rcm.7038>, 2014.
- Yu, X., Pan, Y., Song, W., Li, S., Li, D., Zhu, M., Zhou, H., Zhang, Y., Li, D., Yu, J., Wang, X., and Wang, X.: Wet and Dry Nitrogen Depositions in the Pearl River Delta, South China: Observations at Three Typical Sites With an Emphasis on Water-Soluble Or-

- ganic Nitrogen, *J. Geophys. Res.-Atmos.*, 125, e2019JD030983, <https://doi.org/10.1029/2019JD030983>, 2020.
- Yuan, W., Huang, R.-J., Shen, J., Wang, K., Yang, L., Wang, T., Gong, Y., Cao, W., Guo, J., Ni, H., Duan, J., and Hoffmann, T.: More water-soluble brown carbon after the residential “coal-to-gas” conversion measure in urban Beijing, *npj Clim. Atmos. Sci.*, 6, 20, <https://doi.org/10.1038/s41612-023-00355-w>, 2023.
- Zeng, Y., Ning, Y., Shen, Z., Zhang, L., Zhang, T., Lei, Y., Zhang, Q., Li, G., Xu, H., Ho, S. S. H., and Cao, J.: The Roles of N, S, and O in Molecular Absorption Features of Brown Carbon in PM_{2.5} in a Typical Semi-Arid Megacity in North-western China, *J. Geophys. Res.-Atmos.*, 126, e2021JD034791, <https://doi.org/10.1029/2021JD034791>, 2021.
- Zhang, B., Shen, Z., He, K., Zhang, L., Huang, S., Sun, J., Xu, H., Li, J., Yang, L., and Cao, J.: Source Profiles of Particle-Bound Phenolic Compounds and Aromatic Acids From Fresh and Aged Solid Fuel Combustion: Implication for the Aging Mechanism and Newly Proposed Source Tracers, *J. Geophys. Res.-Atmos.*, 128, e2023JD039758, <https://doi.org/10.1029/2023JD039758>, 2023a.
- Zhang, H., He, P., Liu, L., Dai, H., Zhao, B., Zeng, Y., Bi, J., Liu, M., and Ji, J. S.: Trade-offs between cold protection and air pollution-induced mortality of China’s heating policy, *PNAS Nexus*, 2, pgad387, <https://doi.org/10.1093/pnasnexus/pgad387>, 2023b.
- Zhang, T., Cao, J. J., Tie, X. X., Shen, Z. X., Liu, S. X., Ding, H., Han, Y. M., Wang, G. H., Ho, K. F., Qiang, J., and Li, W. T.: Water-soluble ions in atmospheric aerosols measured in Xi’an, China: Seasonal variations and sources, *Atmos. Res.*, 102, 110–119, <https://doi.org/10.1016/j.atmosres.2011.06.014>, 2011.
- Zhang, Y.-L. and Cao, F.: Fine particulate matter (PM_{2.5}) in China at a city level, *Sci. Rep.*, 5, 14884, <https://doi.org/10.1038/srep14884>, 2015.
- Zhang, Z., Guan, H., Xiao, H., Liang, Y., Zheng, N., Luo, L., Liu, C., Fang, X., and Xiao, H.: Oxidation and sources of atmospheric NO_x during winter in Beijing based on $\delta^{18}\text{O}$ - $\delta^{15}\text{N}$ space of particulate nitrate, *Environ. Pollut.*, 276, 116708, <https://doi.org/10.1016/j.envpol.2021.116708>, 2021a.
- Zhang, Z., Zhou, Y., Zhao, N., Li, H., Tohniyaz, B., Mperijekumana, P., Hong, Q., Wu, R., Li, G., Sultan, M., Zayan, A. M. I., Cao, J., Ahmad, R., and Dong, R.: Clean heating during winter season in Northern China: A review, *Renew. Sust. Energ. Rev.*, 149, 111339, <https://doi.org/10.1016/j.rser.2021.111339>, 2021b.
- Zhao, D. and Sun, B.: Atmospheric Pollution from Coal Combustion in China, *JAPCA J. Air Waste Ma.*, 36, 371–374, <https://doi.org/10.1080/00022470.1986.10466074>, 1986.
- Zhao, R., Zhang, Q., Xu, X., Wang, W., Zhao, W., Zhang, W., and Zhang, Y.: Effect of photooxidation on size distribution, light absorption, and molecular compositions of smoke particles from rice straw combustion, *Environ. Pollut.*, 311, 119950, <https://doi.org/10.1016/j.envpol.2022.119950>, 2022.
- Zheng, P., Chen, Y., Wang, Z., Liu, Y., Pu, W., Yu, C., Xia, M., Xu, Y., Guo, J., Guo, Y., Tian, L., Qiao, X., Huang, D. D., Yan, C., Nie, W., Worsnop, D. R., Lee, S., and Wang, T.: Molecular Characterization of Oxygenated Organic Molecules and Their Dominating Roles in Particle Growth in Hong Kong, *Environ. Sci. Technol.*, 57, 7764–7776, <https://doi.org/10.1021/acs.est.2c09252>, 2023.